

Review

Nanofibres in Drug Delivery Applications

Samia Farhaj¹, Barbara R. Conway^{1,2}  and Muhammad Usman Ghori^{1,*} 

¹ Department of Pharmacy, School of Applied Sciences, University of Huddersfield, Huddersfield HD1 3DH, UK

² Institute of Skin Integrity and Infection Prevention, Huddersfield HD1 3DH, UK

* Correspondence: m.ghori@hud.ac.uk; Tel.: +44-(0)-1484-256950

Abstract: Over the years, scientists have been continually striving to develop innovative solutions to design and fabricate medicines with improved therapeutic potential. Conventional dosage forms, such as tablets, capsules, and injections, are limited when exploited for advanced therapeutics, such as drug targeting. To cater to these limitations, nanofibres have emerged as novel nanomaterials to provide enhanced bioavailability, targeted drug release, extended drug release profile, minimum toxicity, and reduced dosage frequency, which has indisputably improved patient adherence and compliance. This review will concern understanding the potential of drug-loaded nanofibres in drug delivery while comprehending a detailed description of their different production methods. The literature has been thoroughly reviewed to appreciate their potential in developing nanofibrous-based pharmaceutical formulations. Overall, this review has highlighted the importance, versatility, and adaptability of nanofibres in developing medicines with varied drug release kinetics. Several problems must be resolved for their full commercial realisation, such as the drug loading, the initial burst effect, the residual organic solvent, the stability of active agents, and the combined usage of new or existing biocompatible polymers.

Keywords: nanofibres; techniques; drug delivery; electrospinning; centrifugal spinning; solution blowing



Citation: Farhaj, S.; Conway, B.R.; Ghori, M.U. Nanofibres in Drug Delivery Applications. *Fibers* **2023**, *11*, 21. <https://doi.org/10.3390/fib11020021>

Academic Editor: Alexandru Mihai Grumezescu

Received: 31 December 2022

Revised: 1 February 2023

Accepted: 3 February 2023

Published: 17 February 2023



Copyright: © 2023 by the authors. Licensee MDPI, Basel, Switzerland. This article is an open access article distributed under the terms and conditions of the Creative Commons Attribution (CC BY) license (<https://creativecommons.org/licenses/by/4.0/>).

1. Introduction

In recent years, nanotechnology research has grown massively, earning the epithet ‘tiny science’ [1,2]. The area of nanotechnology concerns the investigation, manipulation, and understanding of the properties of materials at the nanoscale [3]. Over the years, nanomaterials have been considered the centre of technological advancements for pharmaceutical, biomedical, and energy applications [4–6]. The production of structures in the nanometric range has provided groundbreaking developments in the healthcare sector [7]. Among various types of nanostructures that have been produced for practical applications, nanofibres are considered useful owing to their high surface area, porosity, ease of fabrication and excellent mechanical performance [8–10]. Currently, polymeric nanofibres are holding the inimitable limelight [11] due to their potential to address some of the limitations of conventional pharmaceutical formulations [12], which lack exactitude in advanced therapeutics [13]. In addition, they offer a promising solution for designing a drug delivery system in which the location, rate, and timing of drug release need to be controlled to achieve the desired therapeutic effect. Generally, these are solid fibres with a diameter of less than 1 μm (1000 nm) [14], having intrinsic nanoscale properties along with unique functionality (high surface area, high surface area-to-volume ratio, high mass transport, and interconnected nanoporosity) [15–18]. For these special characteristics, nanofibres are considered promising and universal drug delivery systems and can be fabricated using established technologies to attain wide-ranging drug-release kinetics (Figure 1). Nanofibres can also potentially protect the drug from decomposition within the body before reaching the target site. These have been exploited to develop formulations for oral, ocular, topical, transmucosal, and transdermal routes. This review is focused on

appraising and compiling the literature to understand the potential of nanofibres in drug delivery while understanding the various manufacturing techniques [19].

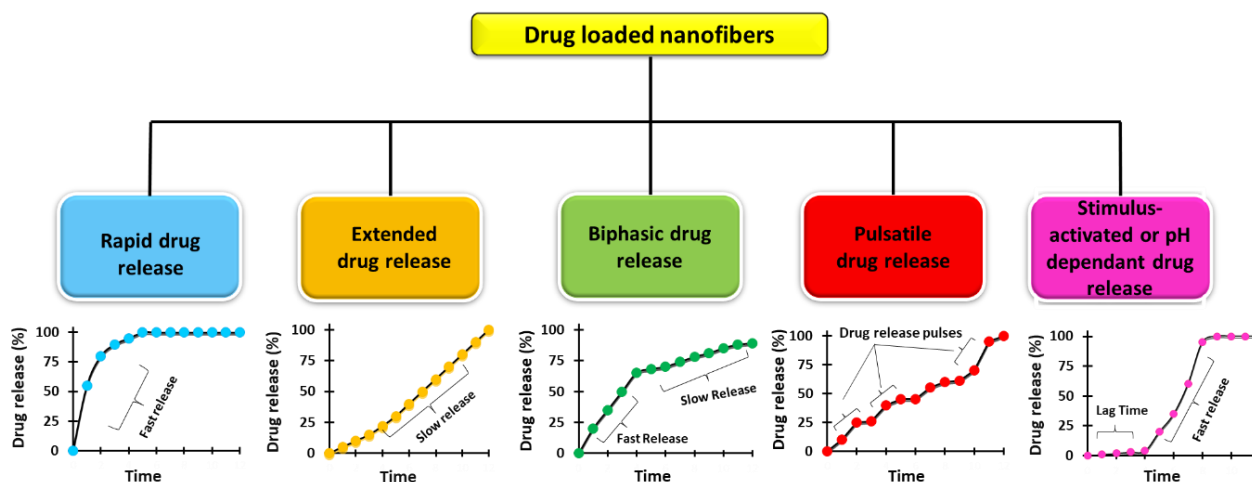


Figure 1. Drug release profiles of various nanofibre-based drug delivery systems.

2. Electrospinning

Electrospinning (ES) is a versatile and robust technique that produces fibres in the micro-to-nanometric range with a controlled surface morphology [20]. The porosity of these nanofibre-based meshes may vary, which can be tailored and controlled by modification of the experimental protocol. In electrospinning, a strong electric field (kV range) is applied to the liquids, which enables them to develop fine-charged jets. These liquids are usually polymer solutions, emulsions, polymer melts, or suspensions containing one or more active pharmaceutical ingredients [21,22]. Based on these liquids' rheological and conductive properties, the applied voltage may change to develop fibres. This technology is considered economical in laboratory and small-scale production [23,24]. It has been exploited for various industrial applications (Figure 2), including biomedical [25], tissue engineering [26], environmental [27], biochemical [28], drug delivery [21], protective clothing [29], and energy storage [30]. In the early 1600s, William Gilbert first reported physical phenomena when he observed spherical drops of water being drawn and deformed into a cone shape or a spray of liquid when a piece of charged amber was placed close to it [31]. There were some notable scientific contributions from C.V Boys (1887), J.F. Cooley (1900 and 1902), W.J. Morton (1902), and John Zeleny (1914), but based on his initial experiments conducted in the 1930s, Anton Formhals (1934–1944) made further notable developments. He patented a setup capable of continuously producing fine nanofibres [32,33]. This period is the real beginning of electrospinning technology. Later, in the 1960s, Geoffrey Taylor investigated the shape of the cone generated under the influence of an electric field with a 49.3° conical angle [34]. This cone was named the '*Taylor cone*', and it has been used widely to explain the process of electrospinning and electrospraying.

Moreover, Taylor also proposed two critical instabilities, i.e., Rayleigh instability and bending instability, which aided in describing the parallel electric field jet phenomena [35]. Later, in the 1990s, Doshi and Reneker reported the development of nanostructured materials using this technique, and attention towards nanotechnology increased dramatically [36,37]. Since then, fibres from electrospinning technology have garnered interest from both industrial and academic sectors. The literature has made tremendous efforts to advance electrospinning technology by investigating mechanisms of fibre-making, characterization of fibres, and exploring novel ways of their applications [5]. Electrospinning involves feeding the spinning fluid in the syringe in the presence of high voltage to establish an electric field between the syringe needle and collector. The polymeric solution at the needle's tip in an electric field becomes electrostatically charged to create a Taylor cone. When surface tension overcomes the electrostatic force, a charged polymer jet is ejected,

which becomes thinner in an accelerated electric field. Additionally, the stretching of the polymer chain and rapid solvent evaporation resulted in solid nanofibres on the collector wall [38]. As shown in Figure 3 [39], the conventional electrospinning setup comprises a precision syringe pump, a high-voltage source, a syringe with a stainless-steel needle, and a collector. The electric supply is connected to the needle and the collector wall, with either a negative or positive charge [40]. The spinnable liquid filled in the syringe is composed of, e.g., a polymer solution with or without an active ingredient known as the working solution [41].

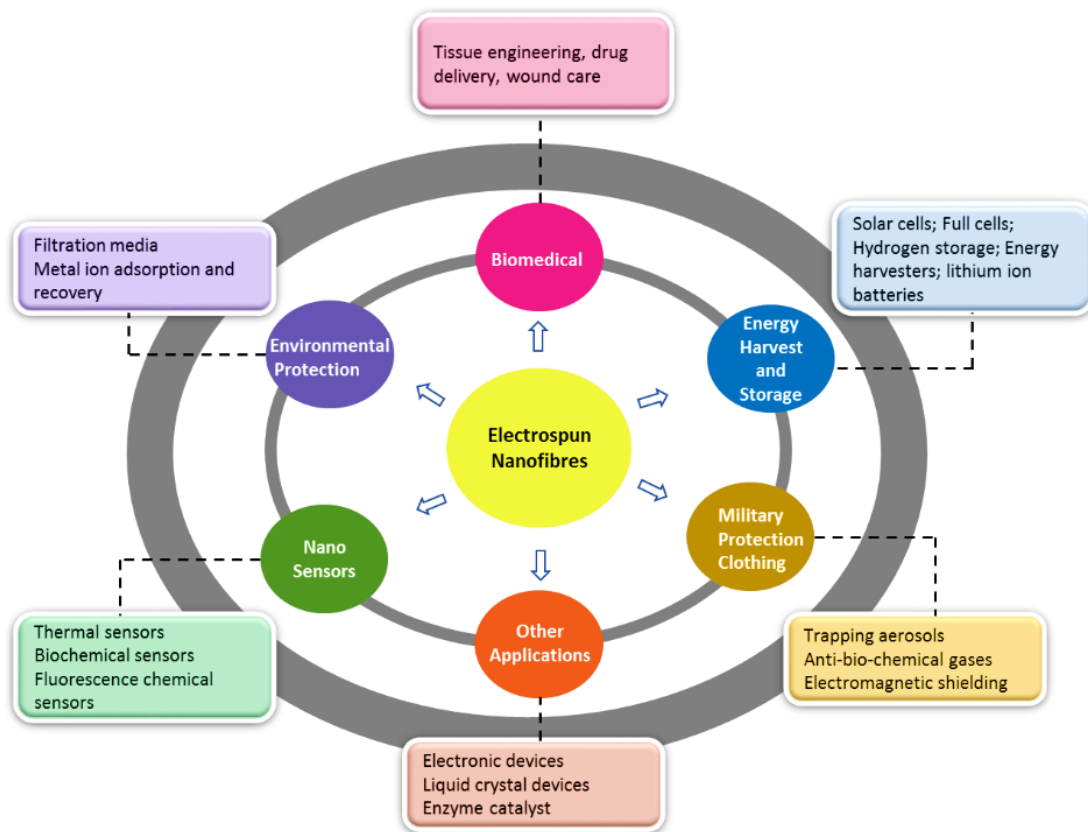


Figure 2. Schematic illustration depicting the various industrial application of electrospinning.

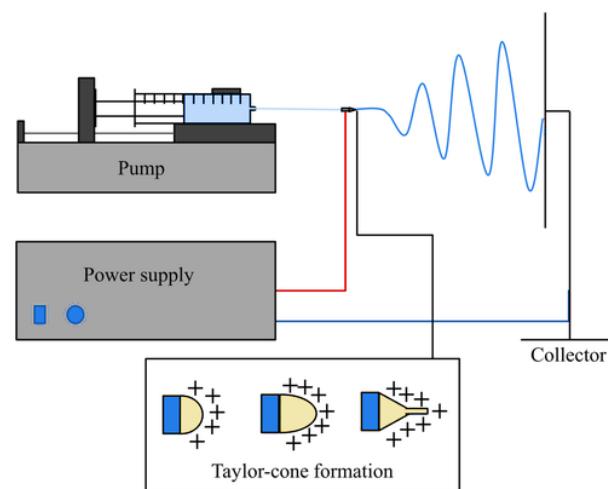


Figure 3. Schematic of a conventional electrospinning setup, reproduced with permission from [38], copyright 2019 Wiley Periodicals, Inc.

2.1. Factors Affecting the Electrospinning Process

The factors affecting electrospinning are classified generally as process, solution, and environmental parameters, as summarised in Table 1. In electrospinning, the process parameters depend upon the applied voltage, flow rate, needle diameter, and distance between the needle and the collector. The parameters of the solution include properties of the solvent used, the concentration of polymer, solution conductivity, and viscosity. The environmental parameters include relative humidity and temperature. All these parameters directly affect the generation of electrospun fibres. In the following section, these are discussed in detail with their implications on the electrospinning process [42].

2.1.1. Effect of Process Parameters

Effect of Applied Voltage

The supplied voltage should be sufficient to initiate jet formation, which mainly depends on the properties of the solution, including viscosity and surface tension. If low voltage is applied, the electrostatic force will be insufficient to overcome the droplet's surface tension; as a result, the jet is not stretched out, and dripping happens. Increasing the voltage beyond the threshold leads to jet formation, which increases the further whipping and instability of fibres, and henceforth, fibre jet elongation occurs [43,44]. The effect of voltage on fibre diameter is controversial. Several studies have reported that increasing the applied voltage decreases fibre diameter [45,46]; however, several other reports discussed a negligible effect or an increase in fibre diameter [47,48].

Effect of Flow Rate

Flow rate, or infusion rate, is the speed at which the spinning solution is propelled towards the spinneret. The rate of solution ejection depends on the inner orifice diameter of the spinneret, applied voltage, and the rate of flow of the solution into the spinneret. Optimum flow rates are needed for any given voltage for any polymer material to produce fibres. When the flow rates are higher than the optimum range, the fibre diameter increases, impacting uniformity [49]. Faster flow rates usually produce coarser nanofibres at a given voltage because more solution is drawn out simultaneously. Additionally, the produced fibres may have defects, such as wrinkles or beads, before reaching the collector if enough time is not given to the solvent for evaporation. However, if the flow rates are lower than the optimum range, the electrospinning process can become intermittent due to the solution depletion at the tip of the nozzle [50,51].

Effect of Distance between Needle and the Collector

The distance between the needle tip and collector also plays an important role in controlling the morphology of the electrospun nanofibres. The morphology of nanofibres can be affected easily by the distance because it depends on the evaporation rate, deposition time, whipping, and instability interval [52]. Therefore, a critical distance must be maintained to develop uniform and smooth electrospun nanofibres [53]. Numerous researchers have studied the effect of the distance between the tip of the needle and collector and concluded that large diameter and defective nanofibres are produced when the distance is small. In contrast, the diameter of fibres is decreased when the distance is enhanced [52,54]. However, in some studies, no direct effect on the fibre's morphology was observed when the distance between the metallic needle and collector was changed [55].

Table 1. Effects of different parameters on the morphology of fibres during the process of electrospinning [56].

Parameters	Effect on Fibre Morphology
Increases in applied voltage	Increase/decrease in fibre diameter
Increase in flow rate	Increase in fibre diameter also leads to (beads on fibre) in case of high flow rate
Increase distance from needle to collector	Electric field unstable, difficulties in performing process
Concentration of polymer	Increase in fibre diameter with increase in concentration
Viscosity	Low generation of beads, high increase in fibre diameter
Solution conductivity	Decrease in fibre diameter with increase in concentration
Solvent volatility	Fibres exhibit micro texture (pores on the surface of fibres, which increase their surface area)

2.1.2. Solution Parameters

In the electrospinning technique, the polymer solution’s viscosity depends primarily on the concentration of the polymer and the type of solvent used. Viscosity is considered a critical parameter because it controls the solutions’ spinnability and its effect on the entanglement of the polymeric molecules for the formation of a continuous polymer jet [57]. However, the polymer solution with low viscosity produces smooth fibres with good mechanical strength and smaller diameters [58]. When the solution has very low viscosity, the polymeric molecules will not be adequately entangled, so beads or drops might be produced instead of fibres after spinning. In another scenario, extremely high viscosity will obstruct polymer flow through the capillary, thus preventing nanofibre production due to localized gel formation Figure 4 [59].

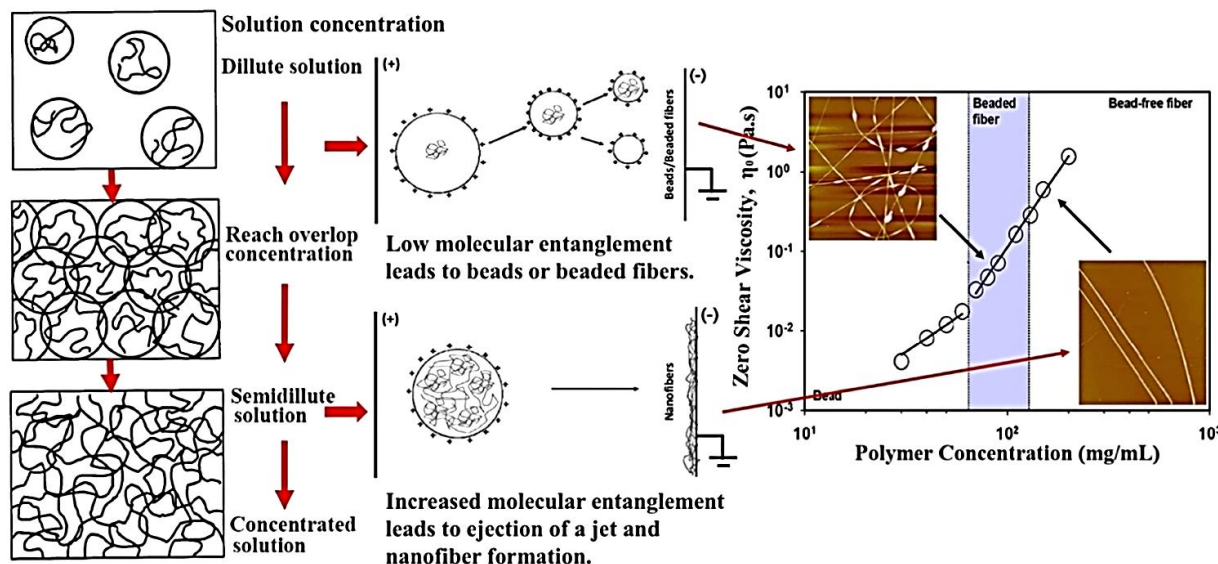


Figure 4. Effect of different polymer concentrations and their molecular entanglement have a direct influence on the morphology of the nanofibres during electrospinning. Reproduced with permission from [60], copyright 2017 Elsevier.

The solvent must be volatile to provide sufficient evaporation when the polymer jet moves towards the collector. The polymer solution is usually fabricated using volatile solvents, which has led to the development of fibres with a high surface area and porous structure. However, if fewer or non-volatile solvents are used, they may lead to the development of fibres having lower surface area and increased pore size, which may be considered less suitable for drug delivery and biomedical applications [59]. Finally, the

conductivity of a polymer solution can also considerably impact the fibres' morphology. Polymer solutions with more substantial conductivity can produce a jet with a greater charge, thus resulting in stronger electrostatic forces. So, the polymer jet experiences greater tensile strength and is stretched more, thus resulting in nanofibres with a smaller diameter and fewer beads [60]. The conductivity of the polymeric solutions can be enhanced by adding polyelectrolytes and ionic salts [41,61,62].

2.1.3. Ambient Conditions

Ambient conditions also play a significant role in the process of electrospinning as high temperature leads to the development of nanofibres with a lower diameter; however, an increase in humidity results in surface pore development [63,64].

3. Types of Electrospinning Techniques and Their Applications in Drug Delivery

3.1. Monoaxial Electrospinning

Monoaxial (or uniaxial) electrospinning is the most prominent method in which the fibres can be made via a single capillary nozzle in the presence of high voltage. Drug delivery systems in monoaxial electrospinning are usually produced using a polymer liquid (typically a solution, suspension, or emulsion). A drug is dispersed in a volatile solvent that can be dragged along with the polymer jet. During the process, higher electrical potential (commonly 5–20 kV) is applied between the needle and the metal collector in the monoaxial electrospinning [65]. The setup of monoaxial electrospinning can be made to spin vertically or horizontally onto a rotating drum or a conduction plate, as illustrated in Figure 5 [53].

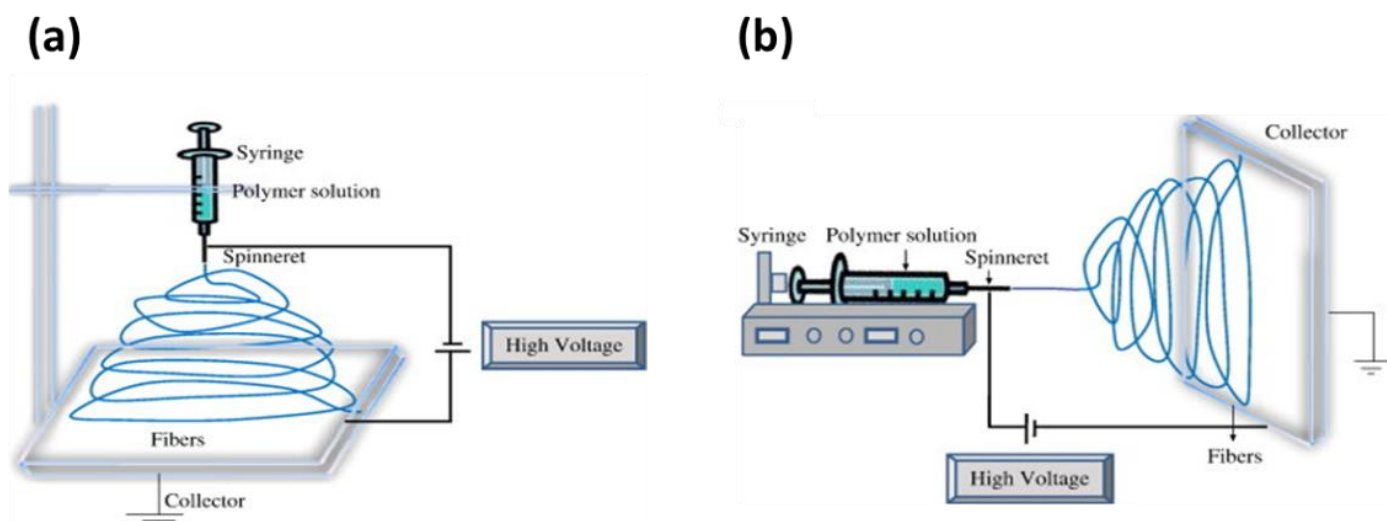


Figure 5. Schematic illustration of setting up of electrospinning apparatus: (a) typical vertical setup and (b) horizontal setup of electrospinning apparatus. Reproduced with permission from [53], copyright 2010 Elsevier.

Application of Monoaxial Electrospinning in Drug Delivery

Electrospinning offers remarkable flexibility in the choice of active ingredients and polymeric materials [67–69] for drug delivery applications. High drug loading capacity (up to 60%) [70–72], high encapsulation efficacy, simultaneous delivery of therapeutic agents, ease of operation, and cost-effectiveness scale [73] are also appealing features in the application of drug delivery, especially for postoperative local chemotherapy and wound-dressing materials [19]. Numerous carrier materials, from natural to synthetic (biodegradable and non-degradable) polymers or a blend of both, have been used successfully for electrospinning [74]. Moreover, drugs that have been investigated for monoaxial ES belong to different classes of therapeutics, like antibiotics [75,76], anticancer drugs [77,78], anti-inflammatory [79], cardiovascular [80,81], and ocular drugs [82,83]. In the following

sections, some studies from the literature have been reported that employed monoaxial electrospinning for drug delivery applications and the summarised characteristics have been tabulated in Table 2.

Electrospun nanofibres have been used successfully to provide a new delivery platform for antibiotic therapy. For instance, Behbood et al. [75] produced chitosan and gelatin electrospun nanofibres to provide a mucoadhesive oral delivery of vancomycin. The prepared fibres were crosslinked with glutaraldehyde to improve the fibrous composites' mechanical properties and water stability. From in vitro dissolution studies, the release of the drug changed from delayed to sustained release, and the dissolution data is best described using the Higuchi mathematical model following diffusion dominated drug release kinetics. In a recent study, a gastro-retentive drug delivery system was developed based on *Bletilla striata* polysaccharide (BSP), a natural polymer. The optimised levofloxacin-loaded BSP lyophilised wafers were coated with polycaprolactone (PCL) electrospun membrane.

The optimised PCL-coated wafer displayed an excellent floating duration of more than 24 h with a sustained drug release profile over an extended time. Both in vitro and in vivo findings illustrated superior performance compared to the pure drug [76]. Additionally, the delivery of electrospun nanofibres of indomethacin to provide a colon-targeted drug delivery after oral administration is evaluated by Akhgari et al. [84]. The formulation comprising Eudragit S:Eudragit RS (60:40) with the 3:5 drug:polymer ratio displayed a pH-responsive drug release. A minor drug release was noticed at pH 1.2, 6.4 and 6.8; however, the bulk of the drug was released at pH 7.4 (simulated colon environment).

Electrospun nanofibres have also found great potential to provide site-specific delivery of chemotherapeutic agents due to their high biocompatibility and tuneable drug release profiles [85]. Therefore, electrospinning has been extensively employed to develop chemotherapeutic delivery systems. Various chemotherapeutic agents, including doxorubicin [77,86], 5-FU [87–91], cisplatin [92–94], paclitaxel [95,96], and metformin [97], have been added as model APIs to determine the ES effectiveness in cancer therapy. For example, Kuang et al. [77] developed doxorubicin (DOX)-loaded polyblend nanofibres to provide a biphasic release of drugs for localised cancer treatment. The release of the drug was tuned in two stages. In the first stage, fast release of the drug was observed to suppress the tumour growth, and in a later stage, nanofibres exhibited sustained release to prolong the adequate therapeutic time. The polymeric blend, which provides a desired release profile of fibres, was composed of 90% PLLA and 10% PEO. In in vivo studies, the localised biodistribution of the drug was observed within the tumour region with no adverse effects. In another study, PCL and chitosan were used to develop electrospun nanofibres loaded with 5-fluorouracil (5-FU). The drug-loaded nanofibres with a high chitosan proportion displayed a sustained release profile for a more extended period than other mats, as shown in Figure 6. Thus, nanofibrous composites can be used as a potential candidate in the treatment of colorectal cancer [78]. Similarly, in a recent study, PCL/gelatin fibres loaded with 5-FU were developed, which increased the amount of gelatin in the blend, and the release of the drug increased. The chemotherapeutic-loaded nanofibres showed suitable cell attachment and HT-29 colorectal cancer cell proliferation whilst displaying a controlled drug release [89].

In recent years, there has been a growing interest in fabricating electrospun nanofibres composed of either natural or synthetic polymers through an electrospinning technique for wound dressing fabrication [98]. For instance, Alavarse et al. [99] developed tetracycline hydrochloride (TCH)-loaded PVA/chitosan fibrous mats for wound dressing. The produced fibrous mats exhibited a burst delivery in the initial 2 h with an effective antibacterial activity against *E. coli*, *S. aureus*, and *Staphylococci epidermidis*. The in vitro scratch assays and cell viability studies showed that the prepared mats were non-cytotoxic and could be used as a potential candidate for wound healing. In another study, Bakhsheshi-Rad et al. [100] developed gentamycin-loaded chitosan-alginate fibres for wound healing. The prepared mats displayed good antibacterial activity, cell attachment, and in vitro proliferation with enhanced regeneration of mice skin. In another study, moxifloxacin-loaded chitosan/PEO

nanofibres were fabricated to provide enhanced healing and antibacterial efficacy as a wound dressing. The developed fibrous mats displayed good antibacterial activity and effectiveness in wound healing compared to the blank nanofibrous mats [101]. The technique of ES has also found great potential in drug delivery via the ocular route. For instance, Mehta et al. [82] investigated the electrospun fibres using one-step spinning process coatings as a novel approach for drug delivery through contact lenses to enhance the permeation of timolol maleate in the eye. The digital images of the coated and uncoated lens are shown in Figure 7. The resultant fibrous coatings containing PVP, poly (N-isopropyl acrylamide) (PNIPAM), borneol (as permeation enhancer), and the drug displayed 20% more drug release compared to the coatings without permeation enhancer. In another study, the ophthalmic inserts of hyaluronan-based nanofibres for ϵ -polylysine and ferulic acid dual delivery. The ferulic acid was blended with polymers and then cross-linked covalently with ϵ -polylysine after the electrospinning process. The cross-linked ocular inserts displayed in vitro biocompatibility and antibacterial activity with fast erosion, which led both the actives to release within 20 min [83].

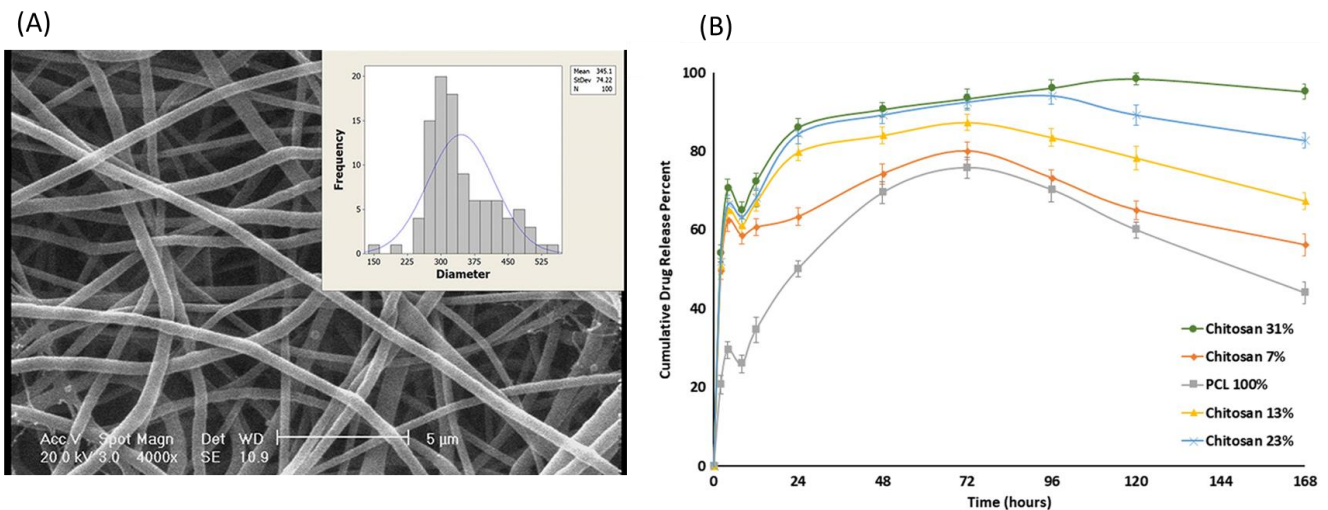


Figure 6. SEM image of nanofibres with (A) sub-figure showing a histogram of fibre diameter distribution (scale 5 μ m) and (B) cumulative release of drug (5-FU) from various nanofibres mat. Reproduced with permission from [78], copyright 2018 John Wiley & Sons, Ltd.

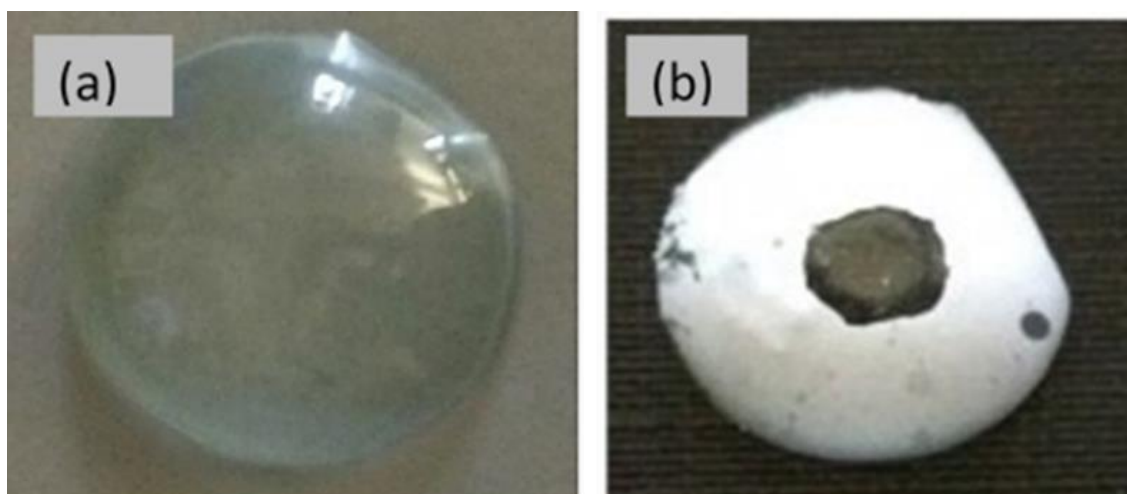


Figure 7. Digital images of uncoated (a) and (b) coated lens. Reproduced with permission from [82], copyright 2017 Elsevier.

Table 2. Summarised characteristics of some studies employing monoaxial electrospinning for drug delivery applications.

Drug(s)	Polymer(s)	Solvent(s)	Drug Release Characteristics	Reference
Vancomycin	Chitosan and gelatin	Glacial acetic acid and water	Sustained drug release	[75]
Levofloxacin	<i>Bletilla striata</i> and PCL	DCM and DMF	Sustained drug release	[76]
Indomethacin	Eudragit RS100 and Eudragit S100	Ethanol	pH-controlled drug release	[84]
Doxorubicin	PEO and PLA	2,2,2-Trifluoroethanol	Biphasic release	[77]
5-fluorouracil	Polycaprolactone and chitosan	Formic acid/acetic acid solution	Sustained drug release	[78]
5-fluorouracil	Polycaprolactone and gelatin	Acetic acid and Formic acid	Controlled drug release	[89]
Tetracycline hydrochloride	PVA and Chitosan	Water and acetic acid solution	Initial burst followed by sustained release	[99]
Ciprofloxacin	PLCL and PNIPAAm	HFIP	Thermosensitive drug release	[102]
Gentamicin	Chitosan and alginate	Acetic acid and DI water	-	[100]
Moxifloxacin	Chitosan and PEO	DI Water	-	[101]
Timolol maleate	PVP and (PNIPAM)	Ethanol	Triphasic drug release	[82]
Ferulic Acid	Hyaluronan and PVP	Ethanol and Water	Burst release	[83]

PCL = Poly(ϵ -caprolactone), PEO = Poly (ethylene oxide), PLA = Poly(lactic acid), PVP = Polyvinylpyrrolidone, PLCL = Poly(l-lactic acid-co- ϵ -caprolactone), PNIPAAm = Poly(N-isopropylacrylamide), DCM = Dichloromethane, DMF = Dime-thylformamide, HFIP = Hexafluoro-2-propanol, DI water = Deionised Water.

3.2. Coaxial Electrospinning

Coaxial electrospinning or (co-electrospinning) encompasses a two-needle spinneret for the development of nanofibres, in which one needle is concentrically inserted inside the other, as illustrated in Figure 8 [103]. Two spinnerets with different or immiscible polymeric solutions pump at varying rates from a single needle port during the coaxial spinning process. The shell solutions flow around the core spinneret (containing the core solution) up to the end of the spinneret until both solutions come in contact and pull towards the collector due to the applied electrostatic potential difference. The core-shell structure is maintained throughout this process, leading to the formation of long core-shell fibrous mats [104]. By applying coaxial electrospinning, multiple drugs can be loaded into the core-sheath fibres, and their release kinetics can be controlled [105].

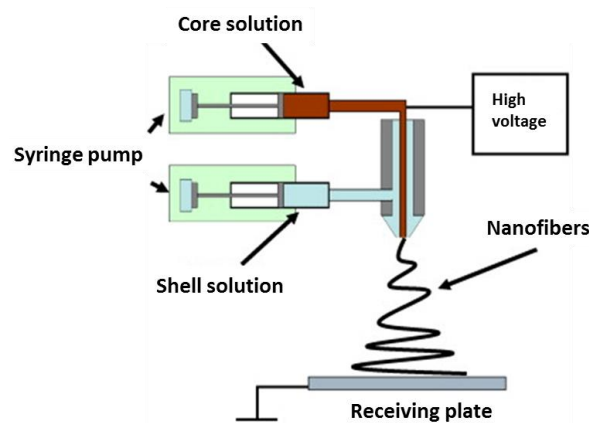


Figure 8. Schematic illustration of a set-up for coaxial electrospinning. Reproduced with permission from [103], copyright 2010 Elsevier.

Applications of Coaxial Electrospinning in Drug Delivery

Coaxial electrospinning provides excellent flexibility in the selection of materials and drugs. Moreover, the modified technique gives high drug encapsulation and enhanced resistance in the protection of bioactives against the harsh environment. The low cost and easy-to-operate setup of coaxial electrospinning make it an appealing system for producing core-shell nanofibres [106]. In the following passages, some studies using coaxial electrospinning in drug delivery are discussed, and their summarised characteristics are tabulated in Table 3.

The core-shell structures obtained from coaxial electrospinning provide a controlled drug release profile in the case of APIs that are water-soluble APIs [107]. For this purpose, coaxially spun fibrous mats, composed of gentamicin/pluronic F127 in the core and silver/PCL in the shells, were developed as sutures to provide drug release in a sustained manner. The *in vitro* release profiles of the scaffolds exhibited an initial burst followed by a sustained release profile for up to 5 weeks, along with no apparent cytotoxicity. Moreover, the drug-loaded scaffolds displayed higher antibacterial activity than nanofibre sutures composed of silver or gentamycin alone [108]. In another study, nanofibrous composites via coaxial ES were developed to provide two drug delivery systems in antitumor applications. For the core structure, a PEG–PLGA emulsion containing Ag or Au and silibinin is used as a therapeutic agent, while PVA containing Fe₂O₃ as magnetic nanoparticles serve as a shell. The nanofibrous structure containing nanoparticles displayed an interesting, sustained release of the drug for more than 60 h without an initial burst [109].

Coaxial electrospinning has also been exploited to fabricate pH-sensitive core-shell nanofibrous composites for the potential delivery of chemotherapeutics in cervical cancer. The core-shell structure PVA and PCL act as a shell, while doxorubicin is embedded in the core. Transmission electron microscope (TEM) analysis determined that the change in flow rate increased the thickness of the shell, as shown in Figure 9a–c. The developed nanofibres exhibited a sustained and pH-responsive release of the drug (Figure 9d,e) with excellent activity against Hela cells of cervical cancer [110].

In a recent study, pH-responsive core-shell nanofibrous mats of PCL and chitosan as a carrier for the delivery of rosuvastatin were reported. The fabricated nanofibres comprised PCL as the core and a chitosan-containing drug as the shell. The cumulative drug release profiles showed an initial burst in the initial stage followed by a slow and sustained release profile over 48 h. The degradation of CS in the shell increased the drug release to 22% at pH 7.4, 64% at pH 6, and 84% at pH 4 after 48 h. From these findings, the PCL/CS fibrous mats can be used as a valuable approach in drug delivery systems [111]. Baghali with his team [112] developed novel core-shell nanofibrous mats for wound healing by incorporating an antibiotic (erythromycin) with appropriate transdermal absorption. The erythromycin-loaded PCL core with zein-containing titanium dioxide (TiO₂) shell nanofibres displayed a sustained release profile for 72 h. Moreover, the prepared nanofibres showed excellent antibacterial activity against gram-positive and negative bacteria. Thus, the novel core-shell nanofibres can be used as an effective biomaterial in wound healing.

The treatment of ocular diseases through solid drug delivery systems has attracted great attention due to their higher potential bioavailability compared to conventional liquid formulations [113]. For this reason, Tawfik et al. [114] reported the development of core-shell nanofibres composed of two drugs. The two different drugs were incorporated in distinct compartments with the aim of treating the abrasion of the cornea and prevent any associated bacterial infection. After the successful development of fibres loaded with moxifloxacin and hydrophilic PVP as the core, the shell was composed of hydrophobic PLGA containing pifrenidone as an antifibrotic drug. The *in vitro* release profile demonstrated an initial burst release of pifrenidone followed by complete drug release after 24 h, while shell moxifloxacin released 60% after 30 min. From these findings, further work to tailor the release profile is required.

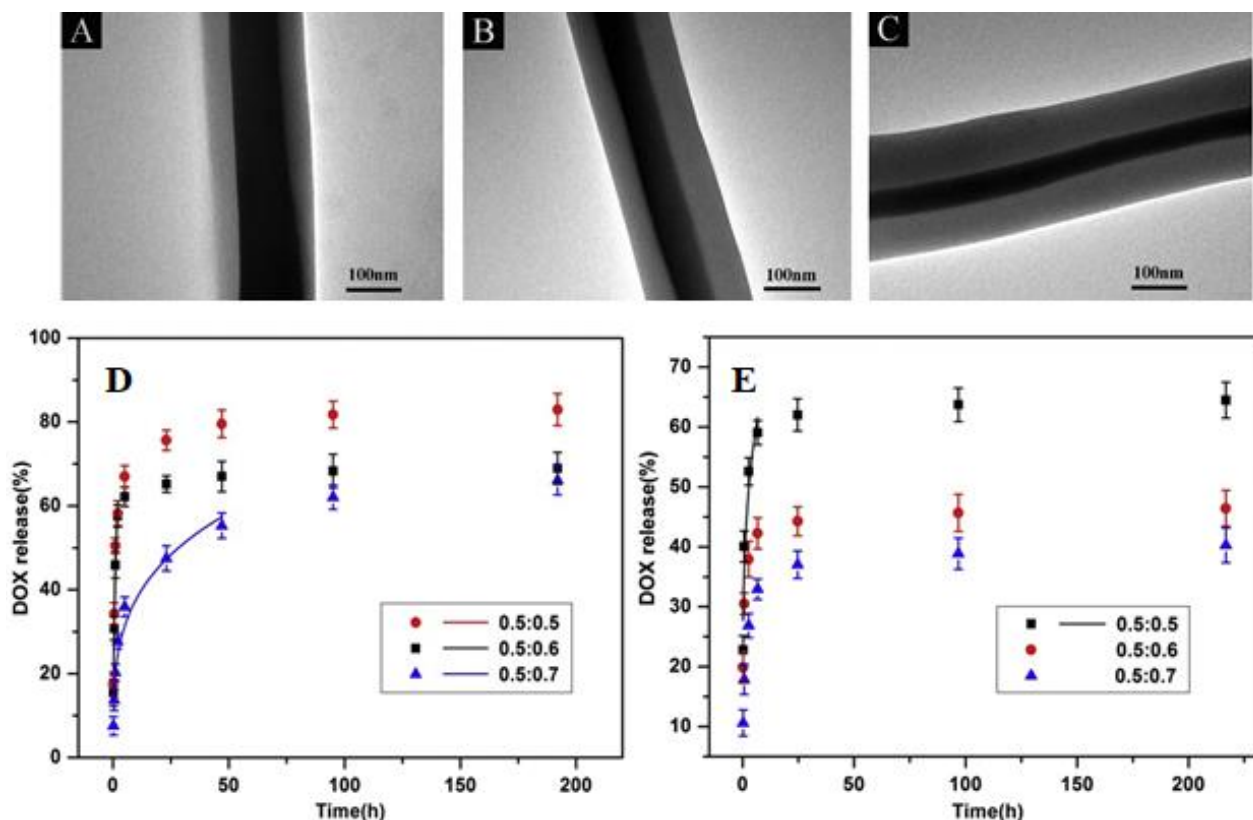


Figure 9. TEM images of the PVA/PCL core-shell nanofibres with flow ratios of 0.5: 0.5 (A), 0.5: 0.6 (B) and 0.5: 0.7 (C), In vitro Drug release profiles of the PVA/PCL core-shell nanofibres in pH = 4 phosphate buffer saline (D), and in pH = 7.4 (E). Reproduced with permission from [110], copyright 2020 Elsevier.

Table 3. Summarised characteristics of studies employing coaxial electrospinning for drug delivery applications.

Drug(s)	Core Fluid	Sheath Fluid	Solvent(s)	Drug Release Characteristics	Reference
Gentamicin	PCL and Pluronic® F-127	Silver and PCL	DCM and DMF	Initial burst followed by Sustained drug release	[108]
Silibinin	PEG-PLGA with Ag or Au	Fe ₂ O ₃ in PVA	DCM	Sustained drug release	[109]
Doxorubicin	PVA	PCL	Distilled water and 2,2,2-Trifluoroethanol via stirring	pH-responsive drug release	[110]
Rosuvastatin	PCL	Chitosan	Acetic acid	pH-responsive release	[111]
Erythromycin	PCL	Zein with Titanium dioxide nanoparticles	Chloroform and ethanol	Sustained release	[112]
Moxifloxacin	PVP	PLGA	Acetonitrile and ethanol	Initial burst, then sustained drug release	[114]

PCL = Poly(ε-caprolactone), PEG= Polyethylene glycol, PLGA = Poly(lactic-co-glycolic acid), PVA = Polyvinyl alcohol, PVP = Polyvinylpyrrolidone, Fe₂O₃ = Iron oxide, DCM = Dichloromethane, DMF = Dimethylformamide.

3.3. Triaxial Electrospinning

Triaxial electrospinning comprises a spinneret with three concentric needles, shown in Figure 10a,b [115]. Three polymer solutions are transferred through different pumps, which meet at the end of the spinneret tip. During the triaxial process, the deformation of a solution happens into a Taylor cone in the presence of an electrostatic field; thus, a jet emerges from the tip when the surface tension is overcome by the electrostatic force. Then, the jet experiences instability during bending, followed by solvent evaporation and, ultimately, dry fibre deposition on the collector wall [116].

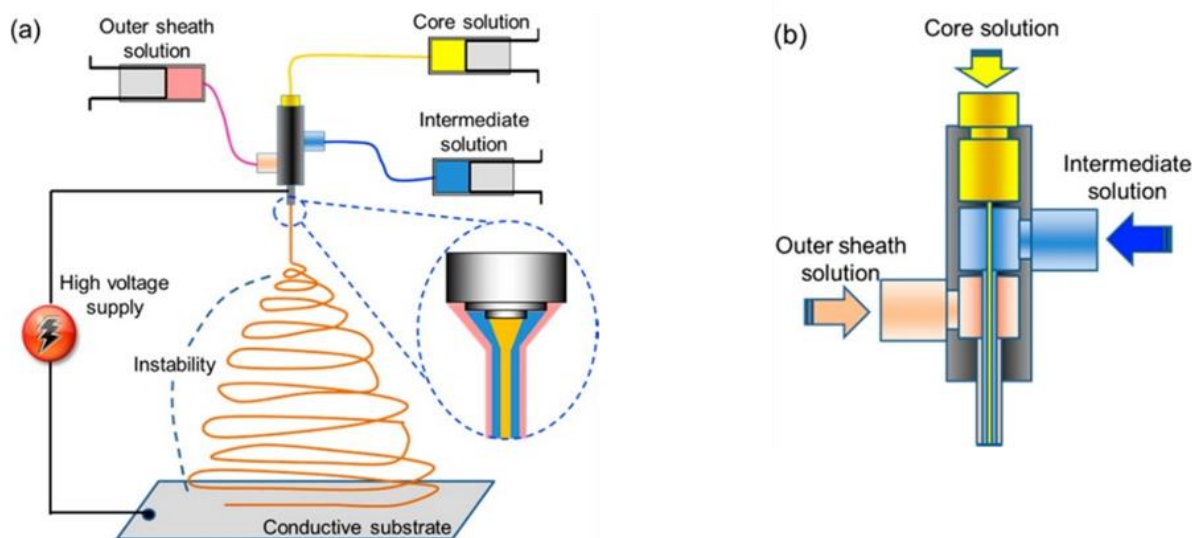


Figure 10. Triaxial electrospinning: (a) basic mechanism, (b) triaxial nozzle. Reproduced with permission from [115]. Copyright 2013 American Chemical Society.

Applications of Triaxial Electrospinning in Drug Delivery

Triaxial electrospinning produces three-layered structure fibrous mats comprising core, intermediate, and shell layers [117]. The technique of triaxial electrospinning is important, particularly when adding hygroscopic material to the shell to acquire excellent biocompatibility. The intermediate hydrophobic layer forces the active molecule from the core via diffusion from the intermediate layer, which provides a sustained release of the drug rather than a premature burst release [115,118]. For triaxial electrospinning, novel carrier vehicles have been investigated to provide a combined delivery of multiple APIs with different release patterns. The dual release from triaxial fibrous composites containing functional molecules [115] can be controlled, or the drug release becomes pH-sensitive from these types of fibres materials [119]. Some of the studies that have been identified as employing triaxial electrospinning are summarised in the subsequent sections and tabulated in Table 4.

The triaxial electrospinning of fibrous composites has been investigated as a method to load different types of drugs along with their different release profiles [120–122]. Triaxial ES also has the advantage of processing a non-spinnable solution for long enough until one of the liquids under the processing phase becomes spinnable. For instance, Yang et al. [123] developed triaxial fibres from a modified triaxial process in which the core liquid contained a solution of sodium diclofenac and lecithin, while the middle layer contained Eudragit S100, and the outer layer contained pure ethanol. In this paper, only the middle liquid was spinnable, which was utilised to obtain triaxial fibres even though the inner fluid was unspinnable, and the outer liquid was pure solvent. The prepared core-shell fibrous mats exhibited a pH-responsive drug release in two successive stages in neutral pH. Initially, dissolution of the shell (ES100) occurred, then release of diclofenac occurred, which led to the enhanced permeation of the drug from intestinal mucosa. Jouybari et al. [124] developed triaxial nanofibres to attain a simultaneous release of three chemotherapeutic

agents. The triaxial nanofibres are composed of chitosan/PVA as the core with 5-FU, while the intermediate layer contains PLA/chitosan with doxorubicin, and the outer layer containing PLA and chitosan is loaded with paclitaxel. The triaxial nanofibres exhibited 90% loading efficacy from all three drugs. In vitro studies demonstrated the slowest release of 5-FU from tri-layer mats due to inner core encapsulation. Moreover, the triaxial fibres displayed higher cell growth inhibition along with enhanced attachment to breast cancer cells (MCF-7). In another study, Li et al. [125] developed tri-layered fibrous composites to provide a time-programmed delivery of multiple anticancer drugs. The tri-axial layers contained glycerol and doxorubicin (Dox) in the inner core, while PCL and PLLA loaded with apatinib (multidrug resistance inhibitor) formed the double walls of the fibrous mats. The rupture of the cavity assured the Dox burst release to reduce the tumour mass, whereas the slow fibre mat degradation ensured a sustained apatinib release to eliminate the tumour. Moreover, in vivo studies demonstrated a synergistic effect in which a time-programmed release of the drug displayed excellent therapeutic effectiveness with no significant toxicity. Nagiah et al. [126] fabricated triaxial fibres comprising PCL as a core layer, gelatin as an intermediate layer, and 50:50 PLGA as a sheath layer. The model drugs were incorporated into the sheath and intermediate layers, i.e., Rhodamine B and Fluorescein isothiocyanate–Bovine Serum Albumin conjugate, respectively. The TEM images, as shown in Figure 11, clearly indicate a tri-layer fibrous structure. Interestingly, triaxial fibres not only exhibited dual release of the drug up to 600 h, but they also exhibited excellent tensile properties compared to uniaxial and coaxial fibres.

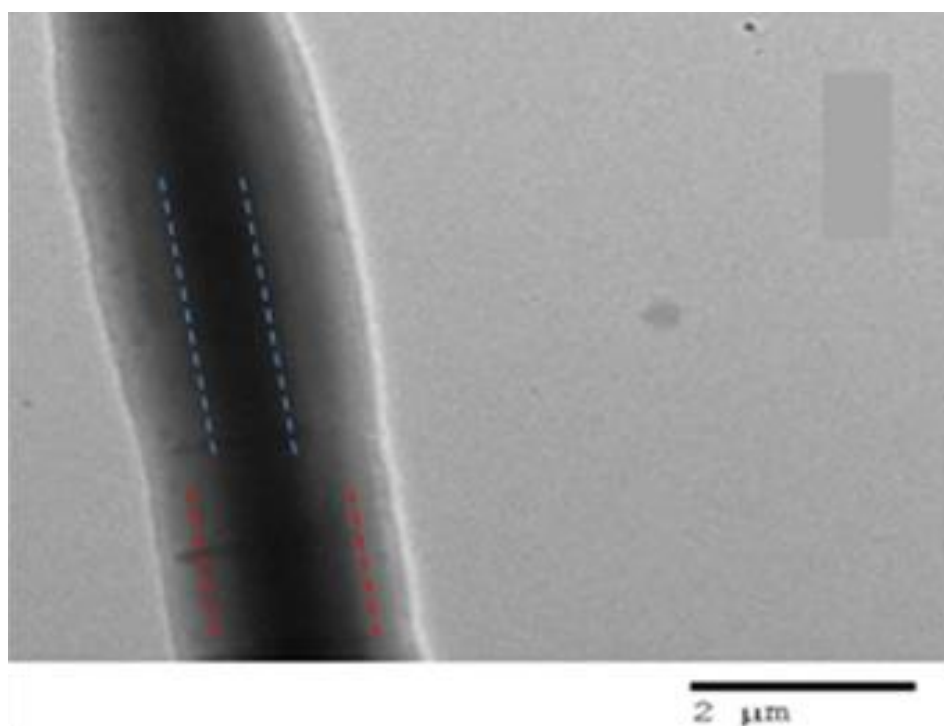


Figure 11. TEM image of Triaxial electrospun fibre with PCL (core, blue dotted line), RhB, BSA-FITC-gelatin (intermediate, red dotted line) layer and PLGA (50:50) (sheath) (scale bar 2 μm). Reproduced with permission from [126], copyright 2020 Scientific Reports.

Ding et al. [127] developed core-shell nanofibres to provide colon-targeted drug delivery in an extended-release manner. The core-shell Eudragit S100 (ES100)-based nanofibres were developed, in which a shell layer ES100 (drug-free) was coated intentionally on a core containing ES100 with aspirin. The developed nanofibrous composites displayed a controlled drug release profile while the drug was freed as an erosion mechanism. The triaxial nanofibres released a smaller portion of the drug in the initial 2 h, protecting the membranes of the stomach and showed extended aspirin release with no significant cytotoxicity.

Table 4. Summarised characteristics of some studies employing triaxial electrospinning for drug delivery applications.

Drug(s)	Core Layer	Intermediate Layer	Sheath Layer	Drug Release Characteristics	Reference
Lecithin and Diclofenac sodium	Lecithin and diclofenac sodium	Eudragit S100	Ethanol	pH-controlled drug release	[123]
5-fluorouracil, Doxorubicin and Paclitaxel	Chitosan/PVA	PLA/Chitosan	PLA/chitosan	Controlled drug release	[124]
Doxorubicin and apatinib	Glycerol	PLLA and PCL		Initial burst followed by sustained drug release	[125]
Rhodamine B and Fluorescein isothiocyanate-Bovine Serum Albumin conjugate	PCL	Gelatin	PLGA	Dual drug release.	[126]
Aspirin	Eudragit (ES100) with Aspirin	Eudragit® S100	Ethanol and DMAc	Extended drug release	[127]

PVA = Polyvinyl alcohol, PCL = Poly(ϵ -caprolactone), PLLA = Poly-(L-lactide); PLA = Polylactic acid, PLGA = Poly(lactic-co-glycolic acid), DMAc = Dimethylacetamide.

3.4. Side-by-Side Electrospinning

In side-by-side electrospinning, two types of polymer solutions are delivered via separate nozzles, which are arranged side-by-side. Both capillaries, from their tips, are connected to a high voltage supply, and the polymer solutions never meet until they reach the capillary end. During the process, when solutions approach the end of the capillary tip, a single Taylor cone is produced from a mixture of the non-uniform solutions, which deposit fibres on the collector wall after solvent evaporation, as shown in Figure 12 [128]. Janus fibres are produced using the side-by-side electrospinning method, comprising two unlike materials on either side of the fibre. For this type of electrospinning, both polymer solutions must possess similar conductivity to develop a single Taylor cone and be expelled in the form of a mixture [129].

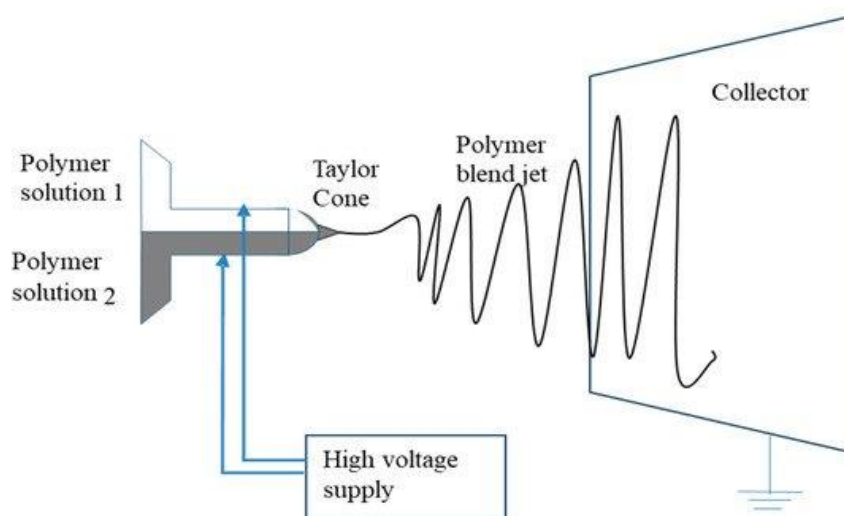


Figure 12. Side-by-side electrospinning schematic diagram. Reproduced with permission from [128], copyright 2019 MDPI.

Applications of Side-by-Side Electrospinning in Drug Delivery

The application of side-by-side electrospinning in the development of Janus fibres for drug delivery is not very frequently employed. Therefore, some of the studies which have been identified are summarised in subsequent sections and tabulated in Table 5.

Table 5. Summarised characteristics some studies employing side-by-side electrospinning for drug delivery applications.

Polymer Solution 1	Polymer Solution 2	Solvent(s)	Drug Release Characteristics	Reference
Ketoprofen and PVP K60	Ethylcellulose, Ketoprofen and PVP k10	Ethanol	Biphasic drug release	[130]
PVP k10	PVP k90, Helicid	DMAc, ethanol	Fast-dissolving drug release	[131]
PVP and ciprofloxacin	Ethylcellulose and silver nanoparticles	Ethanol and acetone	Initial burst followed by sustained drug release	[132]

The first study for the use of side-by-side electrospinning was reported in 2016, in which dual ketoprofen (KET) delivery was achieved through the development of Janus nanofibres. One side of the fibre was composed of PVP, while the other side had ethyl cellulose (EC). The images of the Janus fibres are shown in Figure 13. From in vitro release profile, the PVP side dissolved very fast to unload the dose of KET. At the same time, the EC side provides sustained release of the remaining drug. In conclusion, the application of dual strategy gives robust control over the tuning of the two sides to achieve the maximum therapeutic effect of the APIs [130].

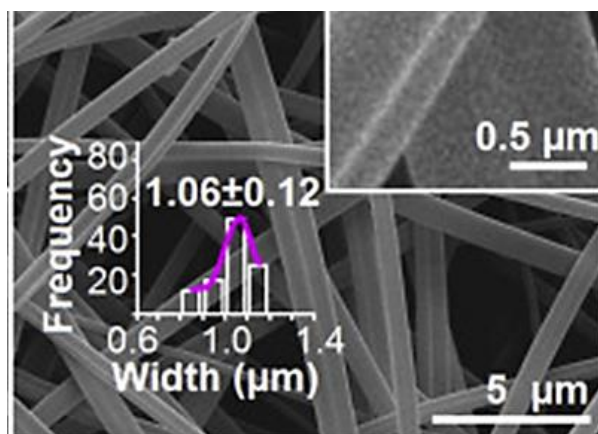


Figure 13. Fibres prepared from side-by-side electrospinning one side composed of PVP while the other side composed of EC, doped with small amount of PVP. Reproduced with permission from [130], copyright 2016 Elsevier.

In another study, Wang with his colleagues developed Janus nanocomposites to improve the oral bioavailability of helicid (a herbal medicine) when administered orally. For the fabrication of Janus fibres, the one spinning solution comprised PVP with the drug. At the same time, the other spinning solution contained a non-spinnable solution along with sodium dodecyl sulphate (a permeation enhancer). The authors successfully spun both solutions simultaneously through the usage of the eccentric spinneret. The TEM image of Janus fibre is shown in Figure 14. The fabricated Janus nanofibres displayed rapid dissolution and an enhanced permeation of helicid on a porcine sublingual mucosa (ex vivo) [131]. In a recent study, nanofibres were developed from PVP and EC polymer matrices through side-by-side electrospinning, in which ciprofloxacin and silver nanoparticles were added to the two sides for wound dressing. Application of the Janus strategy allows the burst

release of ciprofloxacin from the fibres within half an hour. Afterwards, the release of silver nanoparticles was sustained to maintain antibacterial activity for 72 h, thus resulting in potent bacterial growth inhibition [132].

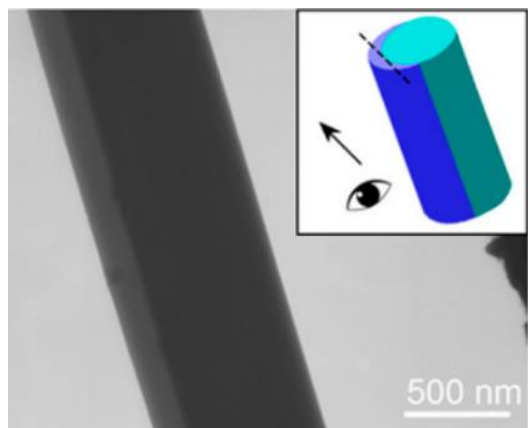


Figure 14. TEM image of the Janus nanofibre. Reproduced with permission from [131], copyright 2018 American Chemical Society.

4. Centrifugal Spinning

Centrifugal spinning, also known as rotary jet or rotary spinning, is an effective method for generating micro- to nanofibres with well-defined structures at low cost and high speed [133]. The technique utilizes centrifugal force to eject polymer jets into fibres instead of electrostatic force so that both conductive and nonconductive polymers can be spun in solution or melts [134]. In the centrifugal spinning process, polymer solutions and emulsions can be added to develop fibres.

4.1. Brief History of Centrifugal Spinning

Centrifugal spinning is not an entirely new technology to the industry. For instance, this technique has been extensively utilised in the production of glass fibres (also known as fibreglass or glass wool) for over half a century [135]. However, the use of this technique to prepare polymeric fibres, particularly polymer nanofibres, is comparatively new. In the 1990s, some big firms, such as BASF Aktiengesellschaft, Owens Corning Fiberglas, and AkzoNobel NV, tried to develop polymer fibres through the centrifugal spinning method. After that, many patents were published discussing spinning heads capable of spinning fibres from polymers. Moreover, the FibeRio Technology Corporation has successfully commercialised a centrifugal spinning system intended for large-scale production [136]. After the rapid popularity and development of centrifugal spinning in the commercial sector, centrifugal spinning also engrossed the interest of academia. In 2008, Weitz and colleagues [137] reported that a 5% solution of poly (methyl methacrylate) (PMMA), after being poured into the middle of a spinning head at 3000 rpm, could develop nanofibres of 25 nm in diameter in a few seconds (Figure 15). It is also reported that the fibre-forming process relies on the competition between the solution's surface tension and centrifugal force.

Lozano and colleagues in 2010, [138] designed a multiple spinning head, which allowed a rotation speed from 3000 to 5000 rpm and produced PEO nanofibres up to 300 nm in diameter. Since 2010, researchers have reported many studies and many polymer solutions have been utilised to develop nanofibres. In 2013, Lu et al. [139] proposed a comprehensive relationship between operational conditions and nanofibre morphology. Numerous academic researchers have published their work employing the centrifugal spinning technique for different applications, including biological materials, energy storage, and photocatalysis [140–143].

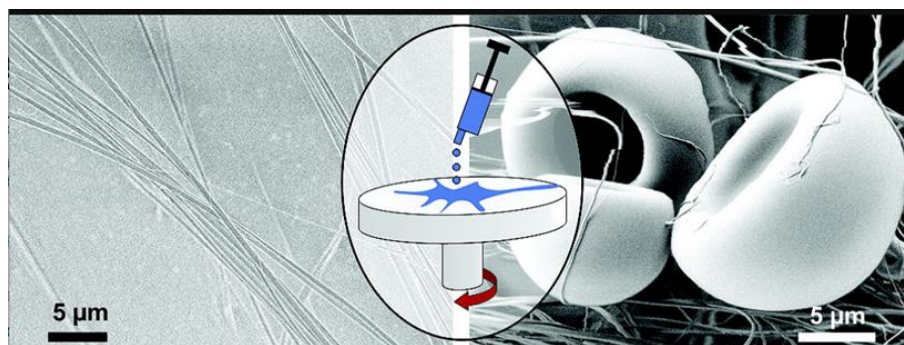


Figure 15. Spinning process and SEM images of the polymethylmethacrylate nanofibre. Reproduced with permission from [137], copyright 2008 American Chemical Society.

4.2. Basic Centrifugal Spinning Mechanism

The basic bench-top centrifugal spinning device is shown in Figure 16 [144]. During the centrifugal spinning process, the solution is fed into the spinning rotating head, which contains several nozzles around the sidewall. As the rotation speed increases to attain a critical value, centrifugal force surpasses the spinning fluid's surface tension; thus, a jet of liquid is emitted from the orifice. At this stage, the liquid jet elongates the solvent, which evaporates simultaneously, until the resultant reaches out towards the collector wall in the form of fibres [135].

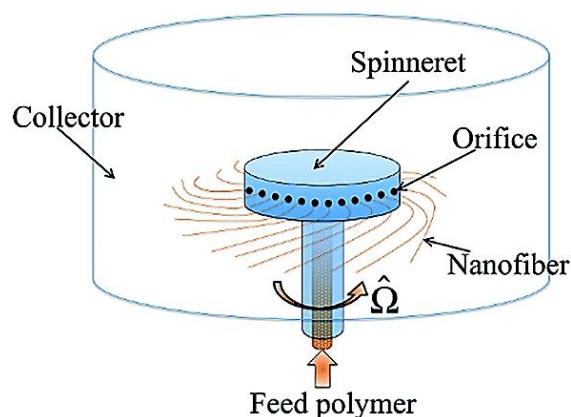


Figure 16. Basic centrifugal spinning system setup. Reproduced with permission from [144], copyright 2014 American Physical Society.

4.3. Effect of Processing Parameters for Fibre Morphology and Diameter

The resultant structure and morphology of nanofibres is affected by a number of aspects of the centrifugal spinning process [145]. Two significant material parameters should be considered during the nanofibre production process, such as the solution's viscosity and surface tension. Besides those, equipment parameters, for instance, the spinneret diameter, and the distance between the collector and the spinneret should also be considered [146]. The process parameters in the centrifugal spinning process, which are critically important, are discussed in the following sections and summarised in Table 6.

Table 6. Effect of different Parameters on centrifugal spinning process [138,147].

Processing parameters	Centrifugal force	Increase in centrifugal force leads to jet breaking and the formation of beads.
	Spinneret angular velocity	Lower angular velocity beads on fibre.
	Orifice radius	Decrease in orifice diameter leads to a decrease in fibre diameter and fewer beads on fibres.
	Distance from spinneret to collector wall	Increase in the distance leads to the breaking of fibre. Decrease in distance leads to increase in fibre diameter.
	Rate of solvent evaporation	Low rate of solvent evaporation leads to collection of fibres in the form of thin film around the collector.
		High rate of evaporation leads to suppression of jet elongation, increase in fibre diameter.
	Temperature of spinneret for meltspun applications	Increase in Temperature cause burning of polymer.
Decrease in temperature leads to an increase in fibre diameter or no jet formation.		
Solution parameters	Viscoelasticity	Increase in viscosity leads to no jet formation Decrease in viscosity leads to beads Formation.
	Concentration of solution	This relates to viscosity of solution which needs to exceed the critical value to attain chain enlargement.
	Surface tension	Decrease in surface tension leads to production of bead fibres

4.4. Viscosity and Surface Tension of the Spinning Solution

In centrifugal spinning, the spinning solution's surface tension and viscosity are considered critical parameters for good fibre formation. The surface tension has a significant role in the development of nanofibre because it is considered the essential force to shrink the surface area of the jet [139]. During the spinning process, the surface tension must be controlled via the centrifugal force to generate a Taylor cone from the spinning solution at the end of the orifice. The surface tension also reduces the surface energy of the solution to avoid droplet formation. The viscosity of the spinning solution is another crucial parameter [148] that also affects the fabrication of nanofibres during centrifugal spinning. If the solution viscosity is too high, the applied forces may not be strong enough to generate a jet. In contrast, the jet will break into droplets or beads if the solution viscosity is very low [149]. The most convenient and reasonable way to monitor the viscosity of the polymer solution is by adjusting the concentration of the polymeric solution [139].

4.5. Spinneret Speed

The speed of the spinneret is also considered a critical parameter for determining the production of nanofibres. During centrifugal spinning, when the speed is low, the centrifugal force cannot overcome the surface tension of the solution, and the solution will be stuck in the spinneret. So, the speed of the spinneret should be appropriate. In a certain range, the diameter of fibres decreases with an increase in spinneret speed. When the rotational speed when reaches a critical limit, the production of fibres will disconnect, resulting in the formation of a lot of beads [139].

4.6. Collection Distance from the Spinneret

The distance between the spinneret and the collector is considered another important parameter because when the distance of the collector changes, the morphology of the nanofibres is not changed, but the nanofibres break more and twist. The distance between the collector and spinneret should decrease when the viscosity of the solution increases. However, if the distance is too short, the fibre will not be allowed to stretch enough; thus,

the diameter of the fibre will be larger. For centrifugal spinning, the optimal collection distance is usually 30–80 cm [150].

4.7. Diameter of the Orifice

The diameter of the orifice determines the solution's flow and the initial diameter of the fibre directly. When the diameter of the orifice is too large, droplet formation happens as a result. When the diameter of the orifice is adequately small, it will result in the formation of nanofibres. Some studies have determined that reducing the orifice diameter decreases the final diameter of the collected nanofibres [151].

4.8. Applications of Centrifugal Spinning in Drug Delivery

Centrifugally spun nanofibres possess a high porosity and surface area; therefore, they have become promising for various applications. In the context of drug delivery, this technique has also gained much attention in the last decade. For instance, Mary et al. [133] developed centrifugally spun PCL/PVP fibres containing tetracycline. The developed fibres were highly aligned with a diameter in the micron range. By varying the concentration of PCL/PVP in the fibres, the drug release can be tuned, and the prepared fibres demonstrated an effective inhibition of bacterial growth. Some of the applications of centrifugal spinning are discussed in subsequent sections and tabulated in Table 7.

The centrifugal spinning technique has also been exploited to develop orodispersible tablets after the compression of microfibrils. The SEM images of carvedilol-loaded rotary spun microfibrils are shown in Figure 17. The *in vitro* dissolution of a poorly soluble drug (carvedilol) was enhanced significantly compared to tablets made from a physical mixture containing the pure drug and hydroxypropyl cellulose. The physical mixture displayed incomplete and pH-dependent drug release profiles [152].

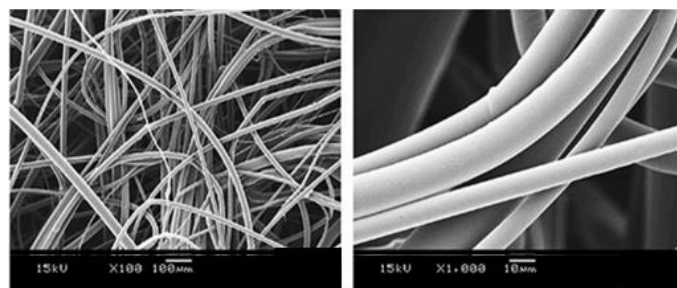


Figure 17. SEM images of carvedilol coating microfibrils. Reproduced with permission from [152], copyright 2015 Elsevier.

To increase the oral bioavailability and solubility of an antipsychotic agent and NSAID (olanzapine and piroxicam, respectively), Marano et al. [153] reported the fabrication of drug-loaded sucrose fibres through the solvent-free method of centrifugal spinning. The fabricated fibres were 10–15 μm in diameter, along with enhanced *in vitro* dissolution performance of the drugs. Another solvent-less study via in-house device was reported by Yang et al. [154], who developed fibrous films of five different drugs (ibuprofen, Indomethacin, tinidazole, nifedipine, and metoprolol tartrate) were developed. The films displayed high drug loadings, highly aligned film structure and orientation with modulable drug release profiles. The centrifugal spinning process enables the development of fibrous structures exhibiting the controlled release of drugs. For instance, Wang et al. [155] reported the development of a PVP fibre loaded with an antibiotic (tetracycline hydrochloride). Upon optimisation of the process, it was possible to obtain fibrous structures with a sustained release of antibiotics. The yielded fibres were in the nanometric range with a slow drug release profile along with good antimicrobial activity. Li et al. [156] fabricated centrifugally spun drug-loaded starch/PEO fibres to improve the solubility and bioavailability of poorly soluble drugs (Ibuprofen and ketoprofen). *In vitro* dissolution profile displayed more than

75% of the drug in the dissolution medium without the initial burst release of the drug. The ibuprofen-loaded fibres displayed sustained drug release over a period of 24 h; however, fibres loaded with ketoprofen did not release the drug for more than 48 h.

Centrifugally spun fibres have found great potential in wound healing due to their high surface area. Therefore, Cremar et al. [157] developed chitosan-based fibrous mats loaded with silver/cinnamaldehyde to provide enhanced antibacterial activity against *S. aureus*. From disk diffusion and cell viability methods, fibrous mats can be used successfully in wound healing due to enhanced antimicrobial activity as shown in Figure 18.

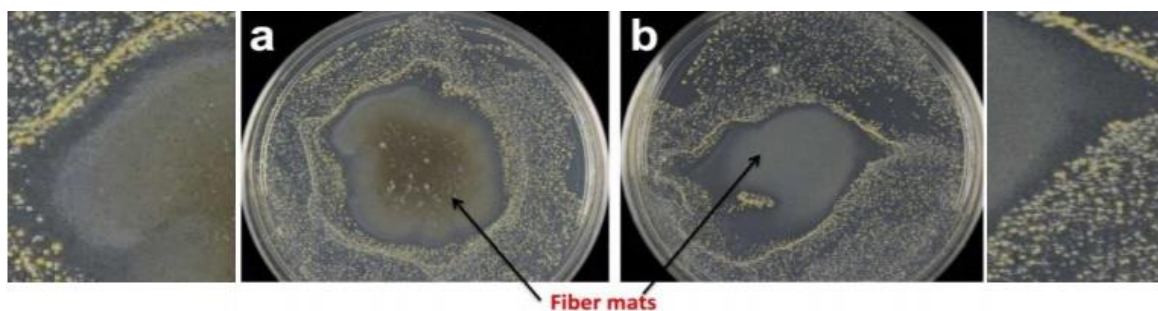


Figure 18. Antibacterial activity of fibrous mats (a) chitosan 0.2% wt with silver nanoparticles and (b) chitosan 0.8% wt with cinnamaldehyde when both were exposed to *Staphylococcus aureus*. The inhibition zone is evident around the mat with both composites. Reproduced with permission from [157]. Copyright 2018 NMJ.

In another study, centrifugally spun fibres were fabricated for wound dressings. The ciprofloxacin loaded PLA/gelatin nanofibres displayed good antimicrobial activity with sustained release of drug up to 1 h (in vitro) [158]. In the same year, Aydogdu et al. [159] successfully developed bacterial cellulose fibres containing a blend of PCL/PLA as an adequate carrier for wound healing. The prepared scaffolds had an exceptional tensile strength and mechanical properties, with the diameter in the range of 5.0–18.5 μm . When researchers use the 70:30 PLA/PCL blend, they can produce fibrous mats like a bandage, which can be used as a potential candidate in wound healing, as shown in Figure 19.

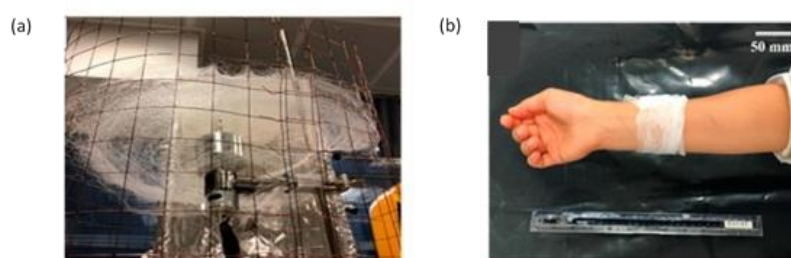


Figure 19. Bandage-like fibrous scaffold fabrication (a) simple centrifugal spinning system (b) image of the prepared sample as wrapped around an arm. Reproduced with permission from [159], copyright 2019 MDPI.

Centrifugal spinning has also found great interest in recent years as a method for tissue engineering. For instance, in 2017, centrifugal spinning was used to develop platelet-functionalised 3D poly- ϵ -caprolactone scaffolds to deliver growth factors. The proposed scaffolds, upon biological evaluation on MG-63 cells, displayed enhanced metabolic activity, alkaline phosphatase activity, and cell proliferation compared to scaffolds that are nonfunctionalized. Moreover, increasing the concentration of platelets in the scaffolds leads to increased cell response due to dose dependency [160]. In another study, 3D fibrous scaffolds were formulated through emulsion centrifugal spinning. The poly- ϵ -caprolactone scaffolds containing growth factors (TGF- β , IGF, and bFGF) enhanced cell proliferation

and chondrogenic differentiation. Thus, the prepared scaffolds can be used as a potential candidate for tissue engineering [161]. In a recent study, force spinning was employed to develop pH-controlled doxorubicin-loaded nanofibres. When functionalised with carbon nano-onions, PCL fibres exhibited a pH-responsive drug release over 15 days: an 87% drug release at pH 6.5 and a 99% drug release at pH 5.0. Thus, from these findings, centrifugally, spin fibrous composites were capable of releasing the drug in a sustained release manner [162].

Table 7. Some of the examples of centrifugal spinning in drug delivery applications.

Drug(s)	Polymer/Carrier	Solvent(s)	Drug Release Characteristics	Reference
Tetracycline	PVP/PCL	Chloroform/ethanol	Rapid drug release followed by sustained drug release	[133]
Carvedilol	Hydroxypropyl cellulose	Ethanol	Rapid drug release	[152]
Olanzapine and piroxicam	Sucrose	-	Fast disintegrating drug release	[153]
Ibuprofen, Indomethacin, tinidazole, nifedipine and metoprolol tartrate	Eudragit [®] EPO, Eudragit [®] RS Polyethylene glycol, Soluplus [®]	-	Modulable drug release	[154]
Tetracycline hydrogen chloride	PVP	Ethanol	Faster drug release followed by controlled drug release	[155]
Platelet	PCL	Chloroform and ethanol	Dose dependant drug release	[160]
Ibuprofen and Ketoprofen	PEO	Water/sodium hydroxide	Fast drug release without initial burst, then sustained drug release	[156]
Cinnamaldehyde or silver	Chitosan	Trifluoroacetic/dichloromethane	-	[157]
Ciprofloxacin	PLA/GE	HFP	Initial burst release of drug followed by sustained drug release	[158]
Bacterial cellulose	PLA/PCL	Chloroform	-	[159]
TGF- β , IGF and bFGF	PCL	Ethanol and chloroform	Prolonged drug release	[161]
Doxorubicin	PCL/PMPMA-CNO _s	Trifluoroacetic acid	Sustained drug release	[162]

TGF- β = Transforming growth factor, IGF = Insulin-like growth factor, bFGF = basic fibroblast growth factor, PVP = Polyvinylpyrrolidone, PCL = Poly(ϵ -caprolactone), PEO = Poly (ethylene oxide), PLA/GE = Poly(lactic acid)/gelatin, HFP = 1,1,1,3,3,3-hexafluoro-2-propanol.

5. Solution and Melt Blowing Spinning

Solution-blowing spinning (SBS) is a new technique to produce polymeric micro/nanofibres from a polymer solution in a process that combines the principle of electrospinning and melt blowing [163]. Solution-blowing spinning necessitates a simple apparatus, homogenous polymer solution in a volatile solvent and a high-velocity gas source [164]. For the spinning device, a specialised nozzle is attached, having an inner nozzle for the pumping of the polymer solution and outer concentric nozzle that to supply pressurised air. During SBS, the streams of the solution are stretched into ultrafine jets under the flow of a high gas velocity from the outer nozzle. Then, the jet is solidified into nanofibres after the evaporation of the solvent Figure 20a,b [165,166].

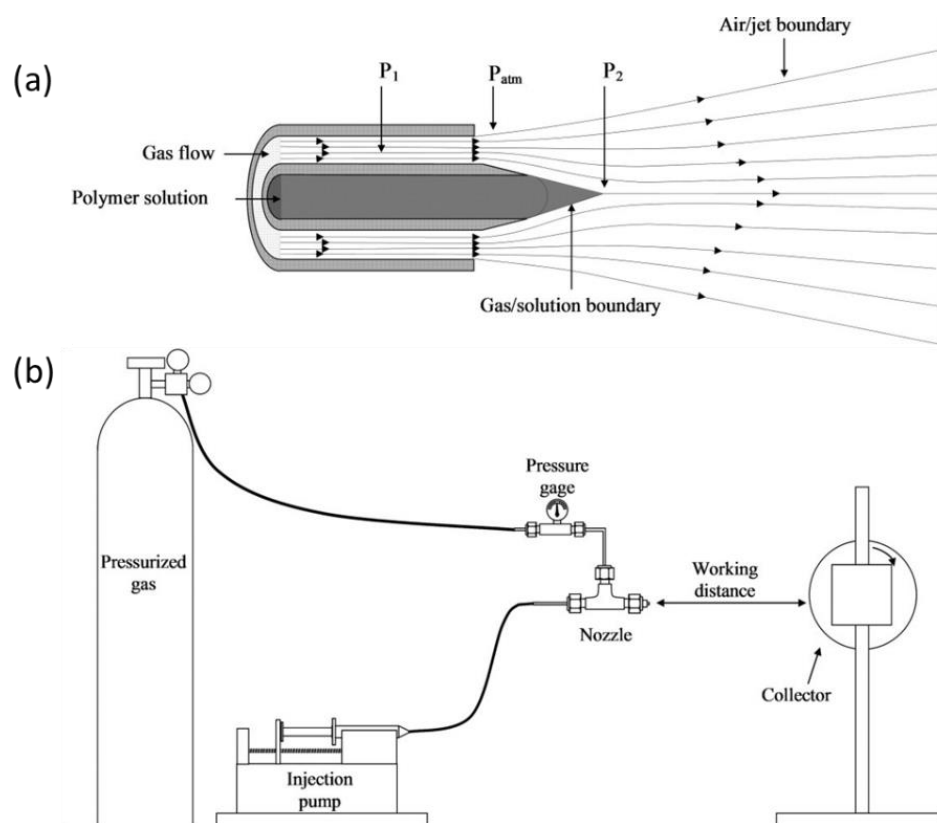


Figure 20. Solution blowing nanofibre system; (a) concentric design of nozzle used in SBS. (b) SBS set-up with a rotating collector. Reproduced with permission from [165], copyright 2020 Elsevier.

5.1. Factors Affecting Solution Blowing and Melt Blowing Spinning

The parameters governing the solution-blowing method have been determined by many researchers. The jet attenuation of the polymer is affected by the number of events during solution blowing, including stretching, instability during bending, flapping motion, and solvent evaporation. In addition, polymer concentration and type also impart a direct morphological effect on the fibre. The injection rate of the solution, the pressure of the gas flow, the protrusion length of the inner nozzle, and the distance from the nozzle to the collector are some of the additional parameters that are important in solution blowing. Table 8 summarises the core parameters that affect the process of fibre formation when employing this technique [167].

Table 8. Factors affecting the solution-blowing process [147].

Parameters	Effect on Fibre Morphology	
Solution parameters	Viscosity	Increase in viscosity low beads formation but increase in fibre diameter.
	Polymer concentration	Polymer concentration is more than 15 wt%, fibre diameter increases.
		Low molecular concentration leads to no sufficient chain entanglement thus cause beads on fibre.
	Molecular weight	Increase leads to decrease in beads formation
	Surface tension	Decrease leads to increase in number of beads.
Vapour pressure		

Table 8. Cont.

Parameters		Effect on Fibre Morphology
Process parameters	Air pressure	Cause great effect on the web uniformity. Decrease in air pressures cause droplets on fibres. No direct influence on diameter of fibre
	Distance between nozzle to collector	The optimum working distance is 30 cm. When the distance is short thin film of nanofibre is generated around the collector due to insufficient solvent evaporation.
	Flow rate of solution	Increase in flow rate cause increase in fibre diameters with greater polymer droplets.
System parameters	Nozzle diameter and geometry	Decrease in nozzle diameter decreases fibre diameter. Nozzle geometry lowers the pressure around inner nozzle, which helps in drawing of polymer solution in cone shape
Ambient conditions	Temperature Humidity Atmospheric pressure	Increase in temperature leads to decrease in fibre diameter. Increase in humidity small spherical pores appear further increase in humidity the pores will be connected. When humidity is very low, solvent evaporation occurs fast. The air flow above the needle, increase evaporation rate resulting in larger fibre diameter.

5.2. Applications of Solution- and Melt-Blowing in Drug Delivery

The solution-blowing method is independent of solvent limitations and electrostatic constraints, so voltage-sensitive polymers can be used without difficulty. These characteristics are causing solution-blowing applications ultimately to be extended from energy to filtration products. In terms of drug delivery, since its first report in 2009 [168], fewer studies have been reported in terms of drug delivery using solution-blowing. The first study was reported by Oliveira and co-workers [169], who prepared PLA fibres which are loaded with the hormone progesterone to provide controlled delivery of drugs in livestock. Initially, fibres were developed from the solutions containing PLA 6% *w/w* and progesterone between 0 and 8% *w/w*, as shown in Figure 21a. In terms of drug release, nanofibres obeyed first-order kinetics, which could potentially be used in controlled drug delivery to control the reproductive cycle in livestock animals (Figure 21b). Some other studies have been discussed in succeeding sections and tabulated in Table 9 employing SBS in drug delivery.

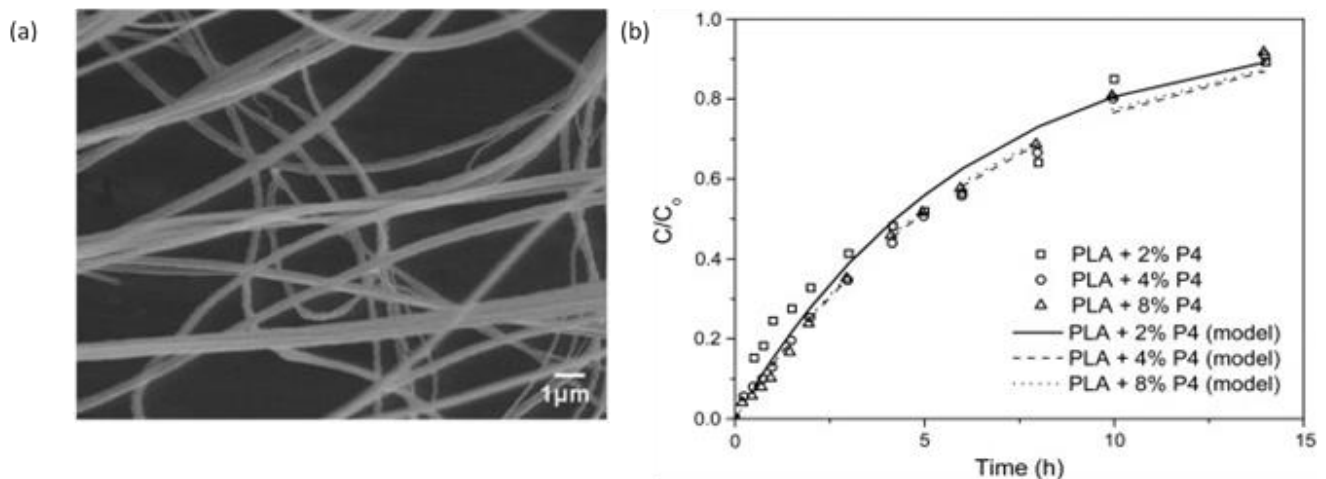


Figure 21. Fibres loaded with progesterone. (a) SEM images of fibres with 6% *w/w* PLA solution containing acetone: chloroform solvent with progesterone 4% *w/w* (b) Progesterone release profiles from fibres prepared from solutions containing PLA 6% *w/v* and 2, 4, or 8%. Reproduced with permission from [169], copyright 2013 Elsevier.

Table 9. Some examples of solution-blowing spinning in drug delivery applications.

Drug(s)	Polymer(s)	Solvent(s)	Type of Drug Delivery	Reference
Progesterone	PLA	Chloroform and acetone	First-order release kinetics	[160]
Diclofenac sodium	PHBV	Hexafluoro isopropanol	Initial burst release followed by controlled drug delivery	[170]
Copaiba oil	PLA/PVP	Chloroform/Acetone	Controlled drug delivery	[171]
Carvedilol	PVPVA64	PEG	Fast drug delivery	[172]

PLA = Poly(lactic acid), PHBV = Poly(3-hydroxybutyrate-co-3-hydroxyvalerate), PVP Polyvinylpyrrolidone, PVPVA64 = Vinylpyrrolidone-vinyl acetate, PEG = Polyethylene glycol.

A study reported a comparison between fibres of PHBV loaded with a drug (sodium diclofenac) prepared with ES and the solution-blowing method. With ES, the drug-loaded fibres had larger diameters compared to the SB fibres. The release profile of the drug was dependent on temperature and drug concentration present within the fibres in both cases [170]. The solution-blowing technique has also been explored to develop fibres from Copaiba oil (CO) obtained from *Copaifera* sp., a medicinal plant often used to provide antimicrobial activity. The composites were constructed from a polymeric blend (PVP and PLA) with a diameter of around 1 μm , as shown in Figure 22a. An increased content of PVP in fibres displayed higher antimicrobial activity against *Staphylococcus aureus* with a controlled release of the drug, as shown in Figure 22b [171].

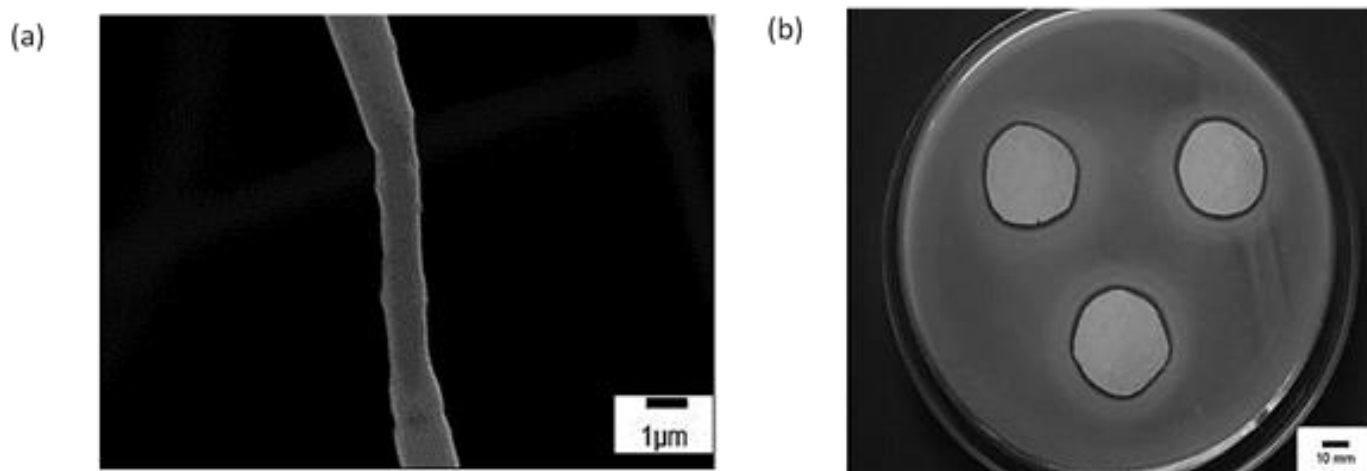


Figure 22. SEM image (a) of Fibres containing PVP and PLA blend with 20-CO (b) In vitro antimicrobial activity of PLA/PVP 20-CO sample against *Staphylococcus aureus*. Reproduced with permission from [171], copyright 2015 Elsevier.

6. Pressurised Gyration

The pressurised gyration (PG)-based hybrid system was first reported in 2013, combining the features of centrifugal spinning and solution-blowing to produce fibres at a large scale with greater control over the final product morphology. The gyration set-up, as shown in Figure 23, essentially contains an aluminium rotary vessel, which is surrounded by pinhole orifices for ejection. The top side of the vessel is connected to a gas inlet for producing pressures of up to 3×10^5 Pa while the bottom part is directly connected with the motor, to rotate the vessel and speed controller rotate the vessel up to 36,000 rpm [173].

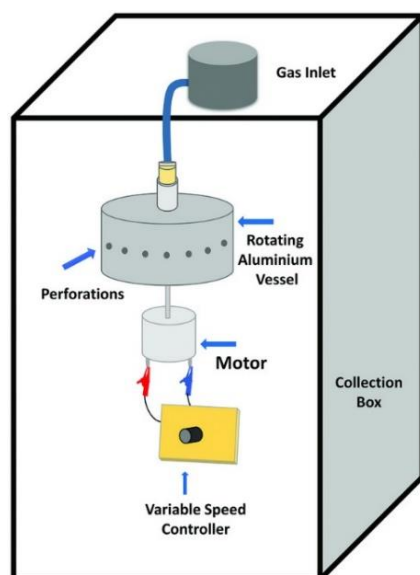


Figure 23. Schematic of pressurized gyration setup. Reproduced with permission from [173], copyright 2018 Wiley-VCH.

6.1. Mechanism of Pressurised Gyration

The PG technique is operated using the Rayleigh–Taylor instability of the chosen polymer solution. The polymer solution is fed into an aluminium rotary vessel, and during the gyration process, when the centrifugal force surpasses the solutions’ surface tension, a jet of liquid is ejected from each pinhole orifice present around the vessel. Fibre formation happens when the polymer jet stretches continuously due to the centrifugal force and the pressure differences arising from the gas inlet near the orifice. During the jetting stage, the solvent evaporates gradually; as a result, fibres are formed around the collector walls in a solid state [173].

6.2. System Parameters of Pressurised Gyration

The formation of fibres mainly depends on the solution properties and processing parameters of the technique. The properties of the solution govern spinnability and ultimately affect the fibre formation process. The applied gas and rotational speed of the vessel are considered critical processing parameters, which produce a marked effect on the morphology of the fibres. In addition, variation in collection distance and environmental conditions also alters the structure of the fibres [173]. Table 10 summarises the parameters of PG on the fibre surface and/or diameter.

Table 10. Factors affecting the pressurised gyration process [173].

	Parameters	Effect on Fibre Morphology
Process parameters	Increase in Working pressure	Decrease in the fibre diameter.
	Increase in spinneret rotating speed	Decrease in the fibre diameter.
Solution parameters	Increase in Polymer molecular	Increase in the fibre diameter.
	Increase in polymer concentration	Increase in the fibre diameter.
	Increase in Solvent volatility	Decrease in the fibre diameter. Increase in the pore size of fibre.
System parameters	Increase in size of orifice	Increase in the diameter of fibre.
Ambient	Increase in Temperature	No direct effect.
	Increase in relative Humidity	Cause decrease in the fibre uniformity.

6.3. Applications of Pressurised Gyration in Drug Delivery

The process of PG provides an attractive manufacturing route for the development of fibres with low diameters, which have demonstrated great potential in drug delivery. The PG technique overcomes major challenges in manufacturing large-scale micro/nanofibrous drug delivery systems, thus providing the production rate in kilograms per hour. In the following paragraphs, the applications of PG in drug delivery have been summarised and tabulated in Table 11.

The process of PG has been used to develop fibres of a poorly soluble drug (ibuprofen) to enhance its dissolution performance. After PG, the PVP fibres alone had diameters in the nanoscale, whereas, after the inclusion of the drug, the fibres were found in the microscale range. The amorphous drug–polymer composites had an accelerated dissolution profile under sink conditions, while non-sink conditions displayed supersaturation [174]. Brako et al. [175] employed PG to prepare a progesterone-loaded nanofibre from a bioadhesive polymer for vaginal therapy. The SEM images and diameter of drug-loaded fibres with 5 wt% of a drug is shown in Figure 24a,b. The hydrophobic drug, after dispersion into hydrophilic polymeric nanofibres (PEO and CMC), displayed a comparable dissolution profile with commercially available Cyclogest (progesterone pessary), as shown in Figure 24c, but nevertheless, the release was observed over 4 h. In conclusion, the PG technique has provided a successful loading of a poorly soluble drug along with suitable release characteristics and morphological properties. The prepared progesterone-loaded fibres have proved to be a promising candidate for drug delivery into the membrane of the vaginal mucosa. More recently, progesterone-loaded poly(lactic) acid polymeric scaffolds were fabricated using both ES and PG techniques to facilitate intra-vaginal therapy. The loaded drug patches obtained from both methods had similar thermal and release characteristics. However, patches attained using ES were more uniformly arranged with smaller fibre diameters in contrast to PG. However, PG provided superior tensile strength in patches and a high production yield compared to ES [176].

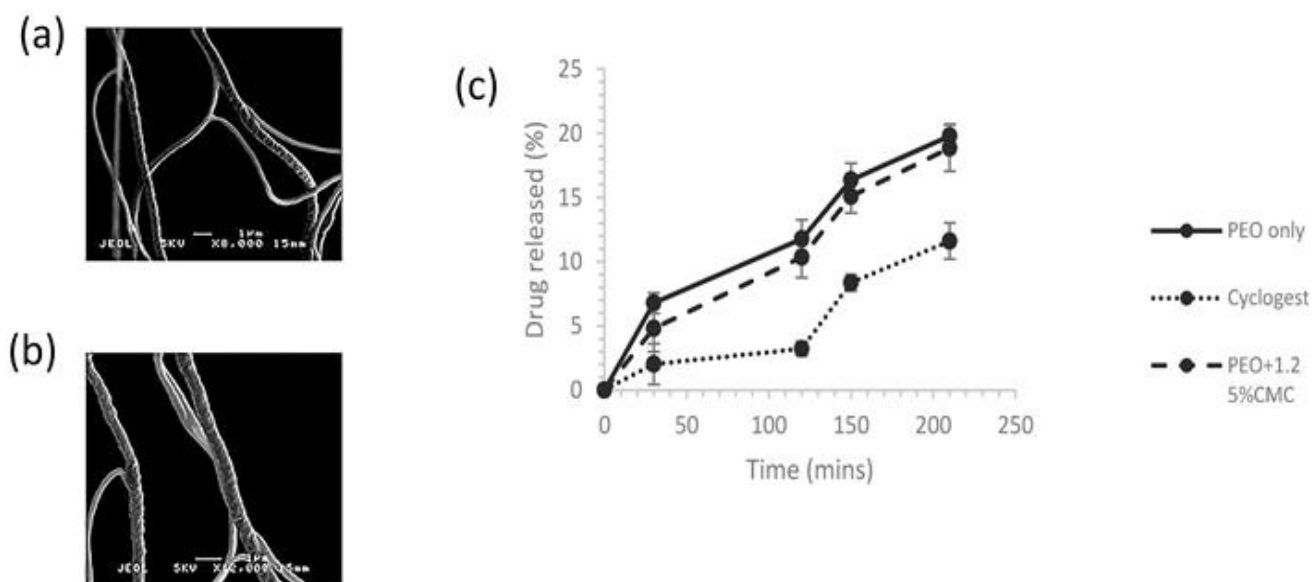


Figure 24. SEM images of (a) progesterone-loaded PEO fibres (produced from a solution containing 5% wt. progesterone and 15% wt. PEO), (b) progesterone-loaded PEO/CMC fibres (produced from a solution containing 5% wt. progesterone, 13.75% wt. PEO and 1.25% wt. CMC), and (c) Progesterone loaded PEO and PEO/CMC fibres and Cyclogest release profiles in stimulated vaginal fluid [175], copyright 2018 Elsevier.

In another study, PG and ES were compared by Ahmed et al. [177] in delivering antifungal agents itraconazole (ITZ) and amphotericin B (AMB) through four spinning polymers PVP, PMMA, PNIPAM, and PVDF. The researchers found that the average

diameter of the fibre was different due to the different types of polymer and methods used. For drug loading, both ITZ and AMB, PVP was selected as an optimal polymer for fibre production. In vitro dissolution studies displayed a successful release of drugs from both types of fibres, with a burst drug release within 15 min from the electrospun fibres. Whereas fibres obtained from PG displayed accelerated dissolution followed by drug release within 5 min and complete drug release in 1 h, as shown in Figure 25.

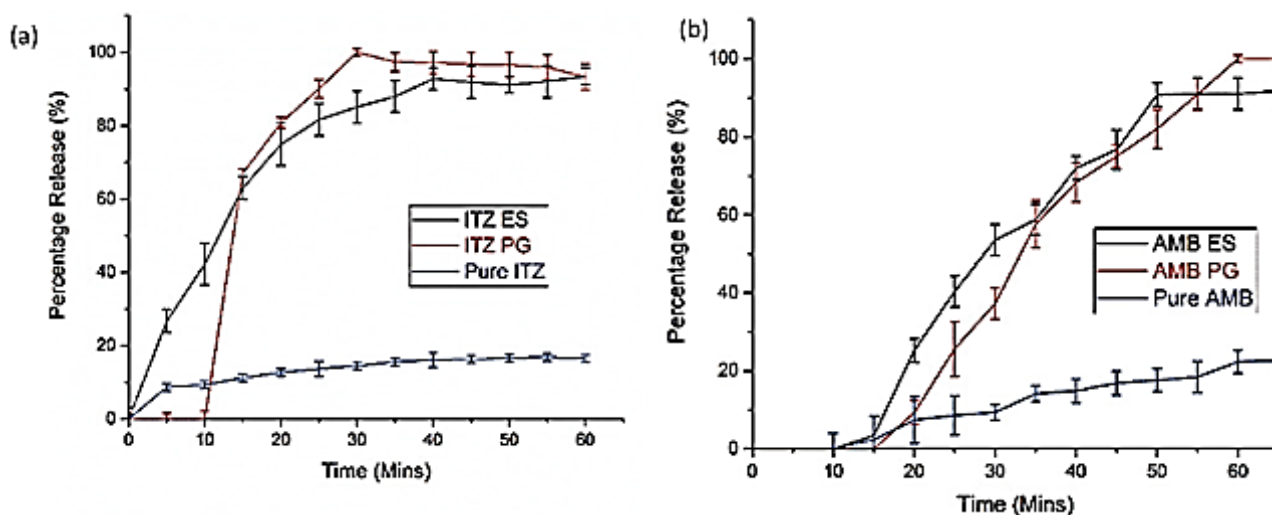


Figure 25. In vitro dissolution profiles of (a) Itraconazole-loaded fibres and (b) amphotericin B fibres. Reproduced with permission from [177]. Copyright 2018 WILEY-VCH.

The use of pressurised gyration in the development of drug-loaded bandages is also found to be very productive in wound healing. For instance, Cinnamon-loaded PCL fibres were engineered and prepared to provide antifungal activity. When fibres were exposed to fungus (*Candida albicans*), no survival was observed after 48 h of treatment. Moreover, after three weeks of the following treatment, no fungal regrowth was seen, thus showing cinnamon efficacy when explored as an antifungal agent [178]. In recent years, the loading of actives to proliferate cells for wound healing has also become an exciting point of interest for researchers. Therefore, in a recent study, pioglitazone hydrochloride (PHR), an insulin-sensitising agent, was loaded into fibrous mats of PVP and PVP/PCL to attain a burst release and a sustained drug release, respectively. From in vitro and in vivo tests, a blend of PCL and PVP in PHR-loaded fibrous mats showed increased activity of epidermal regeneration and fibroblast proliferation, as shown in Figure 26. However, complete oedema improvement and hair follicle formation was only observed in sustained release preparations [179]. More recently, the same researchers developed a combination of pioglitazone with oral antidiabetic (glibenclamide and metformin) nanofibrous scaffolds to accelerate wound healing topically. The triple combination of drugs significantly enhanced epidermal regeneration, i.e., growth of hair follicles was seen within two weeks. Moreover, due to the increased wettability and hydrophilicity of the prepared scaffolds, it was possible to develop sustained release matrices with increased drug bioavailability whilst the dose frequency was reduced [180].

The potential for pressurised gyration in wound healing had also seen great importance when Altun et al. [181] first reported fibres from a blend of bacterial cellulose and PMMA. The produced fibres had an average fibre diameter in the 1.66 to 6.8 μm range. The formulated nanofibres showed no toxicity but enhanced biocompatibility.

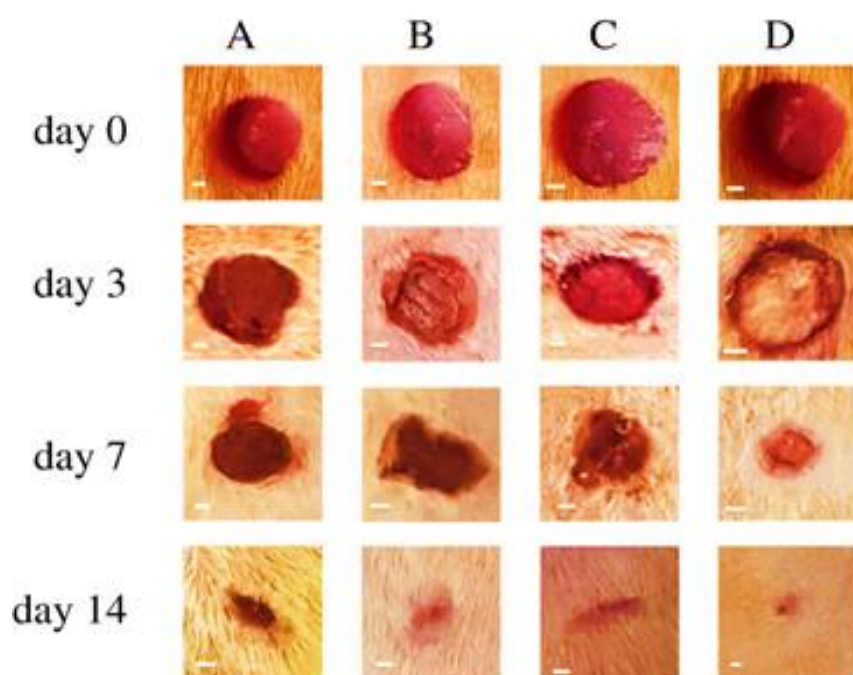


Figure 26. (A) Appearance of wound healing from days 0, 3, 7, and 14 after surgical incision: (A) control group, (B) pure PVP/PCL fibre group, (C) PHR-loaded PVP (12%) fibre group, and (D) PHR-loaded PVP/PCL (12%) fibre group (scale bar = 1 mm). Reproduced with permission from [179], copyright 2020 The Royal Society.

Table 11. Studies in which pressurised gyration has been employed for drug delivery applications.

Drug(s)	Polymer(s)	Solvent(s)	Drug Release Characteristics	Reference
Ibuprofen	PVP	Ethanol	Fast drug release	[174]
Progesterone	PEO and CMC	Ethanol	Zero-order drug release	[175]
Progesterone	PLA	Chloroform	Initial burst release followed by sustained drug release	[176]
Itraconazole and amphotericin B	PVP, PMMA, PNIPAM, and PVDF	Ethanol, dichloromethane, acetone, chloroform, dimethylformamide	Fast drug release	[177]
Cinnamon	PCL	Chloroform	-	[178]
Pioglitazone hydrochloride	PCL and PVP	Ethanol	Depends on the polymer concentration in the fibres. Some showed burst release, while one formulation showed sustained drug release	[179]
Pioglitazone Glibenclamide Metformin	PVP/PCL	Chloroform and methanol	Initial burst followed by sustained drug release	[180]

PVP = Polyvinylpyrrolidone; PEO = Poly (ethylene oxide); CMC = Carboxymethyl cellulose; PMMA = Poly methyl methacrylate; PNIPAM = poly (N-isopropyl acrylamide); PVDF = Polyvinylidene fluoride.

7. Other Techniques

In addition to the techniques discussed already, there are some techniques that have emerged to show the potential to develop nanofibres for drug delivery applications (Table 12). Additional details on the principle of these techniques can be obtained from the recent reviews reported by Qi and Craig [182], Luo et al. [183] for electrospraying, Brown et al. [184] for melt electrospinning, and Cheng et al. [185] for microfluidic spinning.

Table 12. Less commonly employed techniques for drug delivery applications.

Technique	Drugs	Polymers	Solvent(s)/ Excipients	Drug Release Characteristics	Reference
Electrospraying	IGF-1 (growth factor)	PLGA and poly(urethane-urea)	DMSO	Initial burst release followed by slow and subsequently fast drug release	[186]
	Protein bovine serum albumin	PCL and PLGA	Chloroform	Sustained drug release	[187]
	Rhodamine B	PLA/PEO	DCM and DMF	Zero-order drug release	[188]
Melt electrospinning	Carvedilol	Eudragit	-	Fast drug release	[189]
	Carvedilol	Eudragit E	Triacetin, Tween 80, and polyethylene glycol 1500	Fast drug release	[190]
	Curcumin	PCL	DCM/ethanol	Slow drug release without initial burst phase	[191]
Electro blowing	Diclofenac Sodium	HP β CD	Ethanol	Fast drug release	[192]
	Itraconazole	Eudragit E	DCM/methanol	Fast drug release	[193]
Microfluidic spinning	Ampicillin	Alginate	IPA sheath	Extended drug release	[194]

8. Conclusions

In this review, we have discussed the development of nanofibres using different spinning techniques and their applications in drug delivery. The nanofibres produced from monoaxial electrospinning can provide rapid and extended drug release and can target drug delivery in response to pH conditions. Coaxial electrospinning can prepare multifunctional materials. Triaxial spinning offers complicated nano- and microscale architectures with enhanced functional performance, while side-by-side electrospinning was used in the development of Janus fibres for drug delivery. Nanofibres obtained from centrifugal spinning have also been employed in drug delivery along with different carriers, especially polymers. Solution-blowing spinning provides micro–nano scale fibres, while pressurised gyration can generate a large number of homogenous fibres with greater control over final product morphology. Some less well-reported manufacturing techniques have also been discussed. Overall, this review has highlighted the importance, versatility, and adaptability of nanofibres in developing medicines with varied drug release kinetics. Several issues still exist and need to be addressed for their full commercial realisation, such as the drug loading, the initial burst effect, the residual organic solvent, the stability of active agents, and the combined usage of new or existing biocompatible polymers.

9. Challenges and Future Outlook

The emergence of different nanofibre production strategies has led to a substantial breakthrough in developing various platforms for drug delivery technologies. These technologies have made extensive progress in recent years, but not without limitations. Despite noteworthy innovations, many remain in the proof-of-concept stages due to challenges associated with their biopharmaceutical performance. The leading research in electrospinning centrifugal spinning, solution-blowing, and pressurized gyration are moving slowly towards large-scale production, with some systems already being used at the industrial level (e.g., NanoSpinner416n, FibeRio[®] Technology). Although these innovative techniques have shown great potential in developing uniform and continuous fibres, the challenge remains to ensure the production of fibres with the desired mechanical, chemical, and morphological properties, especially during large-scale production. The complex, multifaceted

instrument-related parameters and factors associated with the working solution impact or compromise fibre production. Therefore, optimisation of working conditions and solutions is essential. More importantly, maybe because of these reasons, nanofibres' applications are limited to the laboratory scale, necessitating the need for more in-depth pre-clinical and clinical evaluation to help the translation process of these products to market.

Author Contributions: Conceptualization, M.U.G.; methodology, S.F., B.R.C. and M.U.G.; data curation, S.F., writing—original draft preparation, S.F.; writing—review and editing, S.F., B.R.C. and M.U.G.; supervision, M.U.G.; project administration, M.U.G. All authors have read and agreed to the published version of the manuscript.

Funding: This research received no external funding.

Institutional Review Board Statement: Not applicable.

Data Availability Statement: Not applicable.

Acknowledgments: The authors acknowledge the financial assistance provided by the University of Huddersfield. Samia Farhaj would like to thank the University of Huddersfield for a Fee-Waiver Scholarship for her Ph.D. studies.

Conflicts of Interest: The authors declare no conflict of interest.

References

1. Khan, S.; Mansoor, S.; Rafi, Z.; Kumari, B.; Shoaib, A.; Saeed, M.; Alshehri, S.; Ghoneim, M.M.; Rahamathulla, M.; Hani, U.; et al. A review on nanotechnology: Properties, applications, and mechanistic insights of cellular uptake mechanisms. *J. Mol. Liq.* **2022**, *348*, 118008. [[CrossRef](#)]
2. Fajardo, C.; Martinez-Rodriguez, G.; Blasco, J.; Mancera, J.M.; Thomas, B.; De Donato, M. Nanotechnology in aquaculture: Applications, perspectives and regulatory challenges. *Aquacult. Fish.* **2022**, *7*, 185–200. [[CrossRef](#)]
3. Singh, G.; Kapoor, I.; Dubey, S.; Siril, P.F. Preparation, characterization and catalytic activity of transition metal oxide nanocrystals. *J. Sci. Conf. Proc.* **2009**, *1*, 11–17. [[CrossRef](#)]
4. Kumar, R.; Aadil, K.R.; Ranjan, S.; Kumar, V.B. Advances in nanotechnology and nanomaterials based strategies for neural tissue engineering. *J. Drug Deliv. Sci. Technol.* **2020**, *57*, 101617. [[CrossRef](#)]
5. Sridhar, R.; Lakshminarayanan, R.; Madhaiyan, K.; Barathi, V.A.; Lim, K.H.C.; Ramakrishna, S. Electrospun nanoparticles and electrospun nanofibers based on natural materials: Applications in tissue regeneration, drug delivery and pharmaceuticals. *Chem. Soc. Rev.* **2015**, *44*, 790–814. [[CrossRef](#)] [[PubMed](#)]
6. Shanmugam, V.; Selvakumar, S.; Yeh, C.-S. Near-infrared light-responsive nanomaterials in cancer therapeutics. *Chem. Soc. Rev.* **2014**, *43*, 6254–6287. [[CrossRef](#)]
7. Mehta, P.; Zaman, A.; Smith, A.; Rasekh, M.; Haj-Ahmad, R.; Arshad, M.S.; van der Merwe, S.; Chang, M.-W.; Ahmad, Z. Broad Scale and Structure Fabrication of Healthcare Materials for Drug and Emerging Therapies via Electrohydrodynamic Techniques. *Adv. Ther.* **2019**, *2*, 1800024. [[CrossRef](#)]
8. Ingavle, G.C.; Leach, J.K. Advancements in electrospinning of polymeric nanofibrous scaffolds for tissue engineering. *Tissue Eng. B* **2014**, *20*, 277–293. [[CrossRef](#)]
9. Oliveira, J.E.; Mattoso, L.H.; Orts, W.J.; Medeiros, E.S. Structural and morphological characterization of micro and nanofibers produced by electrospinning and solution blow spinning: A comparative study. *Adv. Mater. Sci. Eng.* **2013**, *2013*, 409572. [[CrossRef](#)]
10. Rezaei, A.; Nasirpour, A.; Fathi, M. Application of Cellulosic Nanofibers in Food Science Using Electrospinning and Its Potential Risk. *Compr. Rev. Food Sci. Food Saf.* **2015**, *14*, 269–284. [[CrossRef](#)]
11. Kajdič, S.; Planinšek, O.; Gašperlin, M.; Kocbek, P. Electrospun nanofibers for customized drug-delivery systems. *J. Drug Deliv. Sci. Technol.* **2019**, *51*, 672–681. [[CrossRef](#)]
12. Tan, E.P.S.; Lim, C.T. Mechanical characterization of nanofibers—A review. *Compos. Sci. Technol.* **2006**, *66*, 1102–1111. [[CrossRef](#)]
13. Patel, G.C.; Yadav, B.K. Polymeric nanofibers for controlled drug delivery applications. In *Organic Materials as Smart Nanocarriers for Drug Delivery*; Patel, G.C., Yadav, B., Eds.; William Andrew Publishing: Norwich, NY, USA, 2018; pp. 147–175.
14. Rahman, M.M. Introductory Chapter: Overview of Nanofibers. In *Nanofiber Research Reaching New Heights*; Rahman, M.M., Asiri, A., Eds.; IntechOpen: London, UK, 2016; pp. 3–8.
15. Unnithan, A.R.; Barakat, N.A.M.; Pichiah, P.B.T.; Gnanasekaran, G.; Nirmala, R.; Cha, Y.-S.; Jung, C.-H.; Newehy, M.E.-N.; Kim, H.Y. Wound-dressing materials with antibacterial activity from electrospun polyurethane–dextran nanofiber mats containing ciprofloxacin HCl. *Carbohydr. Polym.* **2012**, *90*, 1786–1793. [[CrossRef](#)] [[PubMed](#)]
16. Faccini, M.; Vaquero, C.; Amantia, D. Development of protective clothing against nanoparticle based on electrospun nanofibers. *J. Nanomater.* **2012**, *2012*, 892894. [[CrossRef](#)]

17. Sundarrajan, S.; Tan, K.L.; Lim, S.H.; Ramakrishna, S. Electrospun nanofibers for air filtration applications. *Procedia Eng.* **2014**, *75*, 159–163. [[CrossRef](#)]
18. Hrib, J.; Sirc, J.; Hobzova, R.; Hampejsova, Z.; Bosakova, Z.; Munzarova, M.; Michalek, J. Nanofibers for drug delivery—Incorporation and release of model molecules, influence of molecular weight and polymer structure. *Beilstein J. Nanotechnol.* **2015**, *6*, 1939–1945. [[CrossRef](#)]
19. Zahmatkeshan, M.; Adel, M.; Bahrami, S.; Esmaeili, F.; Rezayat, S.M.; Saeedi, Y.; Mehravi, B.; Ashtari, K. Polymer Based Nanofibers: Preparation, Fabrication, and Applications. In *Handbook of Nanofibers*; Barhoum, A., Bechelany, M., Makhoulouf, A., Eds.; Springer International Publishing: Cham, Switzerland, 2018; pp. 1–47.
20. Abdul Hameed, M.M.; Mohamed Khan, S.A.P.; Thamer, B.M.; Rajkumar, N.; El-Hamshary, H.; El-Newehy, M. Electrospun nanofibers for drug delivery applications: Methods and mechanism. *Polym. Adv. Technol.* **2023**, *34*, 6–23. [[CrossRef](#)]
21. Sill, T.J.; Von Recum, H.A. Electrospinning: Applications in drug delivery and tissue engineering. *Biomaterials* **2008**, *29*, 1989–2006. [[CrossRef](#)]
22. Reneker, D.H.; Yarin, A.L. Electrospinning jets and polymer nanofibers. *Polymer* **2008**, *49*, 2387–2425. [[CrossRef](#)]
23. Baji, A.; Mai, Y.-W.; Wong, S.-C.; Abtahi, M.; Chen, P. Electrospinning of polymer nanofibers: Effects on oriented morphology, structures and tensile properties. *Compos. Sci. Technol.* **2010**, *70*, 703–718. [[CrossRef](#)]
24. Mottaghitalab, V.; Haghi, A.K. A study on electrospinning of polyacrylonitrile nanofibers. *Korean J. Chem. Eng.* **2011**, *28*, 114–118. [[CrossRef](#)]
25. Lu, H.; Chen, W.-J.; Xing, Y.; Ying, D.-J.; Jiang, B. Design and preparation of an electrospun biomaterial surgical patch. *J. Bioact. Compat. Polym.* **2009**, *24*, 158–168. [[CrossRef](#)]
26. Nisbet, D.R.; Forsythe, J.S.; Shen, W.; Finkelstein, D.I.; Horne, M.K. A review of the cellular response on electrospun nanofibers for tissue engineering. *J. Biomater. Appl.* **2009**, *24*, 7–29. [[CrossRef](#)] [[PubMed](#)]
27. Bhattarai, S.R.; Bhattarai, N.; Yi, H.K.; Hwang, P.H.; Cha, D.I.; Kim, H.Y. Novel biodegradable electrospun membrane: Scaffold for tissue engineering. *Biomaterials* **2004**, *25*, 2595–2602. [[CrossRef](#)]
28. Li, W.J.; Laurencin, C.T.; Catterson, E.J.; Tuan, R.S.; Ko, F.K. Electrospun nanofibrous structure: A novel scaffold for tissue engineering. *J. Biomed. Mater. Res.* **2002**, *60*, 613–621. [[CrossRef](#)]
29. Lee, S.; Obendorf, S.K. Use of electrospun nanofiber web for protective textile materials as barriers to liquid penetration. *Text. Res. J.* **2007**, *77*, 696–702. [[CrossRef](#)]
30. Thavasi, V.; Singh, G.; Ramakrishna, S. Electrospun nanofibers in energy and environmental applications. *Energy Environ. Sci.* **2008**, *1*, 205–221. [[CrossRef](#)]
31. Tucker, N.; Stanger, J.J.; Staiger, M.P.; Razzaq, H.; Hofman, K. The history of the science and technology of electrospinning from 1600 to 1995. *J. Eng. Fibers Fabr.* **2012**, *7* (Suppl. 2), 63–73. [[CrossRef](#)]
32. Anton, F. Process and Apparatus for Preparing Artificial Threads. U.S. Patent US1975504A, 2 October 1934.
33. Formhals, A. Method and Apparatus for Spinning. U.S. Patent 2,349,950, 2 October 1934.
34. Taylor, G.I. Disintegration of water drops in an electric field. *Proc. R. Soc. Lond. A* **1964**, *280*, 383–397.
35. Taylor, G.I. Electrically driven jets. *Proc. R. Soc. Lond. A* **1969**, *313*, 453–475.
36. Doshi, J.; Reneker, D.H. Electrospinning process and applications of electrospun fibers. *J. Electrostat.* **1995**, *35*, 151–160. [[CrossRef](#)]
37. Kowalewski, T.; Hiller, W.; Behnia, M. An experimental study of evaporating small diameter jets. *Phys. Fluid A* **1993**, *5*, 1883–1890. [[CrossRef](#)]
38. Vass, P.; Szabó, E.; Domokos, A.; Hirsch, E.; Galata, D.; Farkas, B.; Démuth, B.; Andersen, S.K.; Vigh, T.; Verreck, G.; et al. Scale-up of electrospinning technology: Applications in the pharmaceutical industry. *Wiley Interdiscip. Rev. Nanomed. Nanobiotechnol.* **2020**, *12*, e1611. [[CrossRef](#)]
39. Sahay, R.; Thavasi, V.; Ramakrishna, S. Design Modifications in Electrospinning Setup for Advanced Applications. *J. Nanomater.* **2011**, *2011*, 317673. [[CrossRef](#)]
40. He, X.-X.; Zheng, J.; Yu, G.-F.; You, M.-H.; Yu, M.; Ning, X.; Long, Y.Z. Near-field electrospinning: Progress and applications. *J. Phys. Chem. C* **2017**, *121*, 8663–8678. [[CrossRef](#)]
41. Kriegel, C.; Arecchi, A.; Kit, K.; McClements, D.J.; Weiss, J. Fabrication, functionalization, and application of electrospun biopolymer nanofibers. *Crit. Rev. Food Sci. Nutr.* **2008**, *48*, 775–797. [[CrossRef](#)]
42. Haider, A.; Haider, S.; Kang, I.-K. A comprehensive review summarizing the effect of electrospinning parameters and potential applications of nanofibers in biomedical and biotechnology. *Arab. J. Chem.* **2018**, *11*, 1165–1188. [[CrossRef](#)]
43. Ribeiro, C.; Sencadas, V.; Ribelles, J.L.G.; Lanceros-Méndez, S. Influence of processing conditions on polymorphism and nanofiber morphology of electroactive poly (vinylidene fluoride) electrospun membranes. *Soft Mater.* **2010**, *8*, 274–287. [[CrossRef](#)]
44. Beachley, V.; Wen, X. Effect of electrospinning parameters on the nanofiber diameter and length. *Mater. Sci. Eng. C* **2009**, *29*, 663–668. [[CrossRef](#)]
45. Fridrikh, S.V.; Jian, H.Y.; Brenner, M.P.; Rutledge, G.C. Controlling the fiber diameter during electrospinning. *Phys. Rev. Lett.* **2003**, *90*, 144502. [[CrossRef](#)]
46. Megelski, S.; Stephens, J.S.; Chase, D.B.; Rabolt, J.F. Micro- and nanostructured surface morphology on electrospun polymer fibers. *Macromolecules* **2002**, *35*, 8456–8466. [[CrossRef](#)]
47. Gu, S.; Ren, J.; Vancso, G. Process optimization and empirical modeling for electrospun polyacrylonitrile (PAN) nanofiber precursor of carbon nanofibers. *Eur. Polym. J.* **2005**, *41*, 2559–2568. [[CrossRef](#)]

48. Tan, S.-H.; Inai, R.; Kotaki, M.; Ramakrishna, S. Systematic parameter study for ultra-fine fiber fabrication via electrospinning process. *Polymer* **2005**, *46*, 6128–6134. [[CrossRef](#)]
49. Deitzel, J.M.; Kleinmeyer, J.; Harris, D.; Tan, N.B. The effect of processing variables on the morphology of electrospun nanofibers and textiles. *Polymer* **2001**, *42*, 261–272. [[CrossRef](#)]
50. Tang, X.-P.; Si, N.; Xu, L.; Liu, H.-Y. Effect of flow rate on diameter of electrospun nanoporous fibers. *Therm. Sci.* **2014**, *18*, 1447–1449. [[CrossRef](#)]
51. Barua, B.; Saha, M.C. Investigation on jet stability, fiber diameter, and tensile properties of electrospun polyacrylonitrile nanofibrous yarns. *J. Appl. Polym. Sci.* **2015**, *132*, 18. [[CrossRef](#)]
52. Matabola, K.P.; Moutloali, R.M. The influence of electrospinning parameters on the morphology and diameter of poly(vinylidene fluoride) nanofibers-effect of sodium chloride. *J. Mater. Sci.* **2013**, *48*, 5475–5482. [[CrossRef](#)]
53. Bhardwaj, N.; Kundu, S.C. Electrospinning: A fascinating fiber fabrication technique. *Biotechnol. Adv.* **2010**, *28*, 325–347.
54. Wang, T.; Kumar, S. Electrospinning of polyacrylonitrile nanofibers. *J. Appl. Polym. Sci.* **2006**, *102*, 1023–1029. [[CrossRef](#)]
55. Zhang, C.; Yuan, X.; Wu, L.; Han, Y.; Sheng, J. Study on morphology of electrospun poly(vinyl alcohol) mats. *Eur. Polym. J.* **2005**, *41*, 423–432. [[CrossRef](#)]
56. M.Moghadam, S.; Dong, Y.; Barbhuiya, S.; Guo, L.; Liu, D.; Umer, R.; Qi, X.; Tang, Y. Electrospinning: Current Status and Future Trends. In *Nano-Size Polymers*; Fakirov, S., Ed.; Springer: Cham, Switzerland, 2016; pp. 89–154.
57. Jiang, S.; Lv, L.-P.; Landfester, K.; Crespy, D. Nanocounters in and onto Nanofibers. *Acc. Chem. Res.* **2016**, *49*, 816–823. [[CrossRef](#)] [[PubMed](#)]
58. Balaji, A.; Vellayappan, M.; John, A.; Subramanian, A.; Jaganathan, S.; Supriyanto, E.; Razak, S.I.A. An insight on electrospun-nanofibers-inspired modern drug delivery system in the treatment of deadly cancers. *RSC Adv.* **2015**, *5*, 57984–58004. [[CrossRef](#)]
59. Zong, X.; Kim, K.; Fang, D.; Ran, S.; Hsiao, B.S.; Chu, B. Structure and process relationship of electrospun bioabsorbable nanofiber membranes. *Polymer* **2002**, *43*, 4403–4412. [[CrossRef](#)]
60. Liu, G.; Gu, Z.; Hong, Y.; Cheng, L.; Li, C. Electrospun starch nanofibers: Recent advances, challenges, and strategies for potential pharmaceutical applications. *J. Control. Release* **2017**, *252*, 95–107. [[CrossRef](#)] [[PubMed](#)]
61. Son, W.K.; Youk, J.H.; Park, W.H. Preparation of Ultrafine Oxidized Cellulose Mats via Electrospinning. *Biomacromolecules* **2004**, *5*, 197–201. [[CrossRef](#)]
62. Son, W.K.; Youk, J.H.; Lee, T.S.; Park, W.H. Preparation of Antimicrobial Ultrafine Cellulose Acetate Fibers with Silver Nanoparticles. *Macromol. Rapid Commun.* **2004**, *25*, 1632–1637. [[CrossRef](#)]
63. Mit-uppatham, C.; Nithitanakul, M.; Supaphol, P. Ultrafine Electrospun Polyamide-6 Fibers: Effect of Solution Conditions on Morphology and Average Fiber Diameter. *Macromol. Chem. Phys.* **2004**, *205*, 2327–2338. [[CrossRef](#)]
64. Fashandi, H.; Karimi, M. Pore formation in polystyrene fiber by superimposing temperature and relative humidity of electrospinning atmosphere. *Polymer* **2012**, *53*, 5832–5849. [[CrossRef](#)]
65. Gifford-Hollingsworth, R.C. Varying the Porosity of Electrospun Monoaxial and Coaxial Collagen Nanofibers. Master's Thesis, Drexel University, Philadelphia, PA, USA, 2014.
66. Rafiei, S.; Maghsoodloo, S.; Saberi, M.; Lotfi, S.; Motaghitalab, V.; Noroozi, B.; Haghi, A.K. New horizons in modeling and simulation of electrospun nanofibers: A detailed review. *Cellul. Chem. Technol.* **2014**, *48*, 401–424.
67. Ball, C.; Krogstad, E.; Chaowanachan, T.; Woodrow, K.A. Drug-eluting fibers for HIV-1 inhibition and contraception. *PLoS ONE* **2012**, *7*, e49792. [[CrossRef](#)]
68. Blakney, A.K.; Ball, C.; Krogstad, E.A.; Woodrow, K.A. Electrospun fibers for vaginal anti-HIV drug delivery. *Antivir. Res.* **2013**, *100*, S9–S16. [[CrossRef](#)] [[PubMed](#)]
69. Zupančič, Š.; Sinha-Ray, S.; Sinha-Ray, S.; Kristl, J.; Yarin, A.L. Long-term sustained ciprofloxacin release from pmma and hydrophilic polymer blended nanofibers. *Mol. Pharm.* **2016**, *13*, 295–305. [[CrossRef](#)]
70. Chou, S.-F.; Carson, D.; Woodrow, K.A. Current strategies for sustaining drug release from electrospun nanofibers. *J. Control. Release* **2015**, *220*, 584–591. [[CrossRef](#)] [[PubMed](#)]
71. Krogstad, E.A.; Woodrow, K.A. Manufacturing scale-up of electrospun poly(vinyl alcohol) fibers containing tenofovir for vaginal drug delivery. *Int. J. Pharm.* **2014**, *475*, 282–291. [[CrossRef](#)] [[PubMed](#)]
72. Ball, C.; Woodrow, K.A. Electrospun solid dispersions of maraviroc for rapid intravaginal preexposure prophylaxis of HIV. *Antimicrob. Agents Chemother.* **2014**, *58*, 4855–4865. [[CrossRef](#)] [[PubMed](#)]
73. Krogstad, E.A.; Rathbone, M.J.; Woodrow, K.A. Vaginal drug delivery. In *Focal Controlled Drug Delivery*; Domb, A., Khan, W., Eds.; Springer: Boston, MA, USA, 2014; pp. 607–651.
74. Pisani, S.; Dorati, R.; Chiesa, E.; Genta, I.; Modena, T.; Bruni, G.; Grisoli, P.; Conti, B. Release Profile of Gentamicin Sulfate from Polylactide-co-Polycaprolactone Electrospun Nanofiber Matrices. *Pharmaceutics* **2019**, *11*, 161. [[CrossRef](#)]
75. Behbood, L.; Moradipour, P.; Moradi, F.; Arkan, E. Mucoadhesive electrospun nanofibers of chitosan/gelatin containing vancomycin as a delivery system. *J. Rep. Pharm. Sci.* **2017**, *6*, 150.
76. Li, Z.; Zeng, R.; Yang, L.; Ren, X.; Maffucci, K.G.; Qu, Y. Development and characterization of PCL electrospun membrane-coated *Bletilla striata* polysaccharide-based gastroretentive drug delivery system. *AAPS PharmSciTech* **2020**, *21*, 66. [[CrossRef](#)]
77. Kuang, G.; Zhang, Z.; Liu, S.; Zhou, D.; Lu, X.; Jing, X.; Huang, Y. Biphasic drug release from electrospun polyblend nanofibers for optimized local cancer treatment. *Biomater. Sci.* **2018**, *6*, 324–331. [[CrossRef](#)]

78. Hadjianfar, M.; Semnani, D.; Varshosaz, J. Polycaprolactone/chitosan blend nanofibers loaded by 5-fluorouracil: An approach to anticancer drug delivery system. *Polym. Adv. Technol.* **2018**, *29*, 2972–2981. [[CrossRef](#)]
79. Zhao, J.; Cui, W. Fabrication of acid-responsive electrospun fibers via doping sodium bicarbonate for quick releasing drug. *Nanosci. Nanotechnol. Lett.* **2014**, *6*, 339–345. [[CrossRef](#)]
80. Kersani, D.; Mougin, J.; Lopez, M.; Degoutin, S.; Tabary, N.; Cazaux, F.; Janus, L.; Maton, M.; Chai, F.; Sobocinski, J. Stent coating by electrospinning with chitosan/poly-cyclodextrin based nanofibers loaded with simvastatin for restenosis prevention. *Eur. J. Pharm. Biopharm.* **2020**, *150*, 156–167. [[CrossRef](#)] [[PubMed](#)]
81. Bakola, V.; Karagkiozaki, V.; Tsiapla, A.; Pappa, F.; Moutsios, I.; Pavlidou, E.; Logothetidis, S. Dipyridamole-loaded biodegradable PLA nanoplatforms as coatings for cardiovascular stents. *Nanotechnology* **2018**, *29*, 275101. [[CrossRef](#)] [[PubMed](#)]
82. Mehta, P.; Al-Kinani, A.A.; Arshad, M.S.; Chang, M.-W.; Alany, R.G.; Ahmad, Z. Development and characterisation of electrospun timolol maleate-loaded polymeric contact lens coatings containing various permeation enhancers. *Int. J. Pharm.* **2017**, *532*, 408–420. [[CrossRef](#)]
83. Grimaudo, M.A.; Concheiro, A.; Alvarez-Lorenzo, C. Crosslinked Hyaluronan Electrospun Nanofibers for Ferulic Acid Ocular Delivery. *Pharmaceutics* **2020**, *12*, 274. [[CrossRef](#)] [[PubMed](#)]
84. Akhgari, A.; Heshmati, Z.; Afrasiabi Garekani, H.; Sadeghi, F.; Sabbagh, A.; Sharif Makhmalzadeh, B.; Nokhodchi, A. In-dimethacin electrospun nanofibers for colonic drug delivery: In vitro dissolution studies. *Colloids Surf. B* **2017**, *152*, 29–35. [[CrossRef](#)]
85. Chen, Z.; Chen, Z.; Zhang, A.; Hu, J.; Wang, X.; Yang, Z. Electrospun nanofibers for cancer diagnosis and therapy. *Biomater. Sci.* **2016**, *4*, 922–932. [[CrossRef](#)]
86. Jouybari, M.H.; Hosseini, S.; Mahboobnia, K.; Boloursaz, L.A.; Moradi, M.; Irani, M. Simultaneous controlled release of 5-FU, DOX and PTX from chitosan/PLA/5-FU/g-C3N4-DOX/g-C3N4-PTX triaxial nanofibers for breast cancer treatment in vitro. *Colloids Surf. B* **2019**, *179*, 495–504. [[CrossRef](#)]
87. Anothra, P.; Pradhan, D.; Naik, P.K.; Ghosh, G.; Rath, G. Development and characterization of 5-fluorouracil nanofibrous film for the treatment of stomach cancer. *J. Drug Deliv. Sci. Technol.* **2021**, *61*, 102219. [[CrossRef](#)]
88. Esfahani, R.E.; Zahedi, P.; Zarghami, R. 5-Fluorouracil-loaded poly(vinyl alcohol)/chitosan blend nanofibers: Morphology, drug release and cell culture studies. *Iran. Polym. J.* **2021**, *30*, 167–177. [[CrossRef](#)]
89. Ghahreman, F.; Semnani, D.; Khorasani, S.N.; Varshosaz, J.; Khalili, S.; Mohammadi, S.; Kaviannasab, E. Polycaprolactone–Gelatin Membranes in Controlled Drug Delivery of 5-Fluorouracil. *Polym. Sci. Ser. A* **2020**, *62*, 636–647. [[CrossRef](#)]
90. Hu, X.; Liu, S.; Zhou, G.; Huang, Y.; Xie, Z.; Jing, X. Electrospinning of polymeric nanofibers for drug delivery applications. *J. Control. Release* **2014**, *185*, 12–21. [[CrossRef](#)]
91. Son, Y.J.; Kim, W.J.; Yoo, H.S. Therapeutic applications of electrospun nanofibers for drug delivery systems. *Arch. Pharm. Res.* **2014**, *37*, 69–78. [[CrossRef](#)]
92. Aggarwal, U.; Goyal, A.K.; Rath, G. Development and characterization of the cisplatin loaded nanofibers for the treatment of cervical cancer. *Mater. Sci. Eng. C* **2017**, *75*, 125–132. [[CrossRef](#)]
93. Kaplan, J.A.; Liu, R.; Freedman, J.D.; Padera, R.; Schwartz, J.; Colson, Y.L.; Grinstaff, M.W. Prevention of lung cancer recurrence using cisplatin-loaded superhydrophobic nanofiber meshes. *Biomaterials* **2016**, *76*, 273–281. [[CrossRef](#)]
94. Absar, S.; Khan, M.; Edwards, K.; Calamas, D. Electrospinning of cisplatin-loaded cellulose nanofibers for cancer drug delivery. In Proceedings of the ASME 2014 International Mechanical Engineering Congress and Exposition, Montreal, QC, Canada, 14–20 November 2014; p. V009T012A085.
95. Li, B.; Xia, X.; Chen, J.; Xia, D.; Xu, R.; Zou, X.; Wang, H.; Liang, C. Paclitaxel-loaded lignin particle encapsulated into electrospun PVA/PVP composite nanofiber for effective cervical cancer cell inhibition. *Nanotechnology* **2020**, *32*, 015101. [[CrossRef](#)]
96. Chi, H.Y.; Chan, V.; Li, C.; Hsieh, J.H.; Lin, P.H.; Tsai, Y.-H.; Chen, Y. Fabrication of polylactic acid/paclitaxel nano fibers by electrospinning for cancer therapeutics. *BMC Chem.* **2020**, *14*, 63. [[CrossRef](#)]
97. Samadzadeh, S.; Mousazadeh, H.; Ghareghomi, S.; Dadashpour, M.; Babazadeh, M.; Zarghami, N. In vitro anticancer efficacy of Metformin-loaded PLGA nanofibers towards the post-surgical therapy of lung cancer. *J. Drug Deliv. Sci. Technol.* **2021**, *61*, 102318. [[CrossRef](#)]
98. Croitoru, A.-M.; Ficai, D.; Ficai, A.; Mihailescu, N.; Andronescu, E.; Turculet, C.F. Nanostructured Fibers Containing Natural or Synthetic Bioactive Compounds in Wound Dressing Applications. *Materials* **2020**, *13*, 2407. [[CrossRef](#)] [[PubMed](#)]
99. Alavarse, A.C.; de Oliveira Silva, F.W.; Colque, J.T.; da Silva, V.M.; Prieto, T.; Venancio, E.C.; Bonvent, J.-J. Tetracycline hydrochloride-loaded electrospun nanofibers mats based on PVA and chitosan for wound dressing. *Mater. Sci. Eng. C* **2017**, *77*, 271–281. [[CrossRef](#)]
100. Bakhsheshi-Rad, H.R.; Hadisi, Z.; Ismail, A.F.; Aziz, M.; Akbari, M.; Berto, F.; Chen, X.B. In vitro and in vivo evaluation of chitosan-alginate/gentamicin wound dressing nanofibrous with high antibacterial performance. *Polym. Test.* **2020**, *82*, 106298. [[CrossRef](#)]
101. Hameed, M.; Rasul, A.; Nazir, A.; Yousaf, A.M.; Hussain, T.; Khan, I.U.; Abbas, G.; Abid, S.; Yousafi, Q.u.A.; Ghori, M.U. Moxifloxacin-loaded electrospun polymeric composite nanofibers-based wound dressing for enhanced antibacterial activity and healing efficacy. *Int. J. Polym. Mater. Polym. Biomater.* **2020**, *70*, 1271–1279. [[CrossRef](#)]
102. Li, H.; Williams, G.R.; Wu, J.; Wang, H.; Sun, X.; Zhu, L.-M. Poly(N-isopropylacrylamide)/poly(L-lactic acid-co-ε-caprolactone) fibers loaded with ciprofloxacin as wound dressing materials. *Mater. Sci. Eng. C* **2017**, *79*, 245–254. [[CrossRef](#)]

103. Chen, R.; Huang, C.; Ke, Q.; He, C.; Wang, H.; Mo, X. Preparation and characterization of coaxial electrospun thermoplastic polyurethane/collagen compound nanofibers for tissue engineering applications. *Colloids Surf. B* **2010**, *79*, 315–325. [[CrossRef](#)]
104. Sun, Z.; Zussman, E.; Yarin, A.L.; Wendorff, J.H.; Greiner, A. Compound Core–Shell Polymer Nanofibers by Co-Electrospinning. *Adv. Mater.* **2003**, *15*, 1929–1932. [[CrossRef](#)]
105. Vasita, R.; Gelain, F. Core-sheath fibers for regenerative medicine. In *Nanomaterials in Drug Delivery, Imaging, and Tissue Engineering*; John Wiley and Sons: Hoboken, NJ, USA, 2013; pp. 493–533.
106. Lu, Y.; Huang, J.; Yu, G.; Cardenas, R.; Wei, S.; Wujcik, E.K.; Guo, Z. Coaxial electrospun fibers: Applications in drug delivery and tissue engineering. *Wiley Interdiscip. Rev. Nanomed. Nanobiotechnol.* **2016**, *8*, 654–677. [[CrossRef](#)]
107. Tong, H.-W.; Zhang, X.; Wang, M. A new nanofiber fabrication technique based on coaxial electrospinning. *Mater. Lett.* **2012**, *66*, 257–260. [[CrossRef](#)]
108. Chen, S.; Ge, L.; Mueller, A.; Carlson, M.A.; Teusink, M.J.; Shuler, F.D.; Xie, J. Twisting electrospun nanofiber fine strips into functional sutures for sustained co-delivery of gentamicin and silver. *Nanomedicine* **2017**, *13*, 1435–1445. [[CrossRef](#)]
109. Fazio, E.; Ridolfo, A.; Neri, G. Thermally activated noble metal Nanoparticles incorporated in electrospun fiber-based drug delivery systems. *Curr. Nanomater.* **2019**, *4*, 21–31. [[CrossRef](#)]
110. Yan, E.; Jiang, J.; Yang, X.; Fan, L.; Wang, Y.; An, Q.; Zhang, Z.; Lu, B.; Wang, D.; Zhang, D. pH-sensitive core-shell electrospun nanofibers based on polyvinyl alcohol/polycaprolactone as a potential drug delivery system for the chemotherapy against cervical cancer. *J. Drug Deliv. Sci. Technol.* **2020**, *55*, 101455. [[CrossRef](#)]
111. Yousefi, P.; Dini, G.; Movahedi, B.; Vaezifar, S.; Mehdikhani, M. Polycaprolactone/chitosan core/shell nanofibrous mat fabricated by electrospinning process as carrier for rosuvastatin drug. *Polym. Bull.* **2021**, *79*, 1627–1645. [[CrossRef](#)]
112. Baghali, M.; Ziyadi, H.; Faridi-Majidi, R. Fabrication and characterization of core-shell TiO₂-containing nanofibers of PCL-zein by coaxial electrospinning method as an erythromycin drug carrier. *Polym. Bull.* **2022**, *79*, 1729–1749. [[CrossRef](#)]
113. Luraghi, A.; Peri, F.; Moroni, L. Electrospinning for drug delivery applications: A review. *J. Control. Release* **2021**, *334*, 463–484. [[CrossRef](#)] [[PubMed](#)]
114. Tawfik, E.A.; Craig, D.Q.M.; Barker, S.A. Dual drug-loaded coaxial nanofibers for the treatment of corneal abrasion. *Int. J. Pharm.* **2020**, *581*, 119296. [[CrossRef](#)] [[PubMed](#)]
115. Han, D.; Steckl, A.J. Triaxial Electrospun Nanofiber Membranes for Controlled Dual Release of Functional Molecules. *ACS Appl. Mater. Interfaces* **2013**, *5*, 8241–8245. [[CrossRef](#)] [[PubMed](#)]
116. Liu, W.; Ni, C.; Chase, D.B.; Rabolt, J.F. Preparation of multilayer biodegradable nanofibers by triaxial electrospinning. *ACS Macro Lett.* **2013**, *2*, 466–468. [[CrossRef](#)]
117. Huang, C.K.; Zhang, K.; Gong, Q.; Yu, D.G.; Wang, J.; Tan, X.; Quan, H. Ethylcellulose-based drug nano depots fabricated using a modified triaxial electrospinning. *Int. J. Biol. Macromol.* **2020**, *152*, 68–76. [[CrossRef](#)]
118. Nagiah, N.; Murdock, C.J.; Bhattacharjee, M.; Nair, L.; Laurencin, C.T. Development of Tripolymeric Triaxial Electrospun Fibrous Matrices for Dual Drug Delivery Applications. *Sci. Rep.* **2020**, *10*, 609. [[CrossRef](#)]
119. Yang, C.; Yu, D.-G.; Pan, D.; Liu, X.-K.; Wang, X.; Bligh, S.A.; Williams, G.R. Electrospun pH-sensitive core-shell polymer nanocomposites fabricated using a tri-axial process. *Acta Biomater.* **2016**, *35*, 77–86. [[CrossRef](#)]
120. Khalf, A.; Madihally, S.V. Modeling the permeability of multiaxial electrospun poly (ϵ -caprolactone)-gelatin hybrid fibers for controlled doxycycline release. *Mater. Sci. Eng. C* **2017**, *76*, 161–170. [[CrossRef](#)]
121. Yu, D.-G.; Li, X.-Y.; Wang, X.; Yang, J.-H.; Bligh, S.A.; Williams, G.R. Nanofibers fabricated using triaxial electrospinning as zero order drug delivery systems. *ACS Appl. Mater. Interfaces* **2015**, *7*, 18891–18897. [[CrossRef](#)] [[PubMed](#)]
122. Yang, G.-Z.; Li, J.-J.; Yu, D.-G.; He, M.-F.; Yang, J.-H.; Williams, G.R. Nanosized sustained-release drug depots fabricated using modified tri-axial electrospinning. *Acta Biomater.* **2017**, *53*, 233–241. [[CrossRef](#)] [[PubMed](#)]
123. Adepu, S.; Ramakrishna, S. Controlled drug delivery systems: Current status and future directions. *Molecules* **2021**, *26*, 5905. [[CrossRef](#)] [[PubMed](#)]
124. Liu, M.; Zhang, Y.; Sun, S.; Khan, A.R.; Ji, J.; Yang, M.; Zhai, G. Recent advances in electrospun for drug delivery purpose. *J. Drug Target.* **2019**, *27*, 270–282. [[CrossRef](#)]
125. Li, X.; He, Y.; Hou, J.; Yang, G.; Zhou, S. A Time-Programmed Release of Dual Drugs from an Implantable Trilayer Structured Fiber Device for Synergistic Treatment of Breast Cancer. *Small* **2020**, *16*, 1902262. [[CrossRef](#)]
126. Chen, S.; Boda, S.K.; Batra, S.K.; Li, X.; Xie, J. Emerging roles of electrospun nanofibers in cancer research. *Adv. Healthc. Mater.* **2018**, *7*, 1701024. [[CrossRef](#)]
127. Ding, Y.; Dou, C.; Chang, S.; Xie, Z.; Yu, D.-G.; Liu, Y.; Shao, J. Core–Shell Eudragit S100 Nanofibers Prepared via Triaxial Electrospinning to Provide a Colon-Targeted Extended Drug Release. *Polymers* **2020**, *12*, 2034. [[CrossRef](#)]
128. Bhattarai, R.S.; Bachu, R.D.; Boddu, S.H.; Bhaduri, S. Biomedical applications of electrospun nanofibers: Drug and nanoparticle delivery. *Pharmaceutics* **2019**, *11*, 5. [[CrossRef](#)]
129. Gupta, P.; Wilkes, G.L. Some investigations on the fiber formation by utilizing a side-by-side bicomponent electrospinning approach. *Polymer* **2003**, *44*, 6353–6359. [[CrossRef](#)]
130. Yu, D.-G.; Yang, C.; Jin, M.; Williams, G.R.; Zou, H.; Wang, X.; Annie Bligh, S.W. Medicated Janus fibers fabricated using a Teflon-coated side-by-side spinneret. *Colloids Surf. B* **2016**, *138*, 110–116. [[CrossRef](#)]
131. Wang, K.; Liu, X.-K.; Chen, X.-H.; Yu, D.-G.; Yang, Y.-Y.; Liu, P. Electrospun Hydrophilic Janus Nanocomposites for the Rapid Onset of Therapeutic Action of Helicid. *ACS Appl. Mater. Interfaces* **2018**, *10*, 2859–2867. [[CrossRef](#)] [[PubMed](#)]

132. Yang, J.; Wang, K.; Yu, D.-G.; Yang, Y.; Bligh, S.W.A.; Williams, G.R. Electrospun Janus nanofibers loaded with a drug and inorganic nanoparticles as an effective antibacterial wound dressing. *Mater. Sci. Eng. C* **2020**, *111*, 110805. [[CrossRef](#)] [[PubMed](#)]
133. Mary, L.A.; Senthilram, T.; Suganya, S.; Nagarajan, L.; Venugopal, J.; Ramakrishna, S.; Giri Dev, V. Centrifugal spun ultrafine fibrous web as a potential drug delivery vehicle. *Express Polym. Lett.* **2013**, *7*, 238–248. [[CrossRef](#)]
134. McEachin, Z.; Lozano, K. Production and characterization of polycaprolactone nanofibers via forcespinning™ technology. *J. Appl. Polym. Sci.* **2012**, *126*, 473–479. [[CrossRef](#)]
135. Zhang, X.; Lu, Y. Centrifugal spinning: An alternative approach to fabricate nanofibers at high speed and low cost. *Polym. Rev.* **2014**, *54*, 677–701. [[CrossRef](#)]
136. Voelker, H.; Zettler, H.D.; Fath, W.; Berbner, H. Production of Fibers by Centrifugal Spinning. U.S. Patent 5494616A, 27 February 1996.
137. Weitz, R.; Harnau, L.; Rauschenbach, S.; Burghard, M.; Kern, K. Polymer nanofibers via nozzle-free centrifugal spinning. *Nano Lett.* **2008**, *8*, 1187–1191. [[CrossRef](#)]
138. Sarkar, K.; Gomez, C.; Zambrano, S.; Ramirez, M.; de Hoyos, E.; Vasquez, H.; Lozano, K. Electrospinning to forcespinning™. *Mater. Today* **2010**, *13*, 12–14. [[CrossRef](#)]
139. Lu, Y.; Li, Y.; Zhang, S.; Xu, G.; Fu, K.; Lee, H.; Zhang, X. Parameter study and characterization for polyacrylonitrile nanofibers fabricated via centrifugal spinning process. *Eur. Polym. J.* **2013**, *49*, 3834–3845. [[CrossRef](#)]
140. Bao, N.; Wei, Z.; Ma, Z.; Liu, F.; Yin, G. Si-doped mesoporous TiO₂ continuous fibers: Preparation by centrifugal spinning and photocatalytic properties. *J. Hazard. Mater.* **2010**, *174*, 129–136. [[CrossRef](#)]
141. Wang, L.; Shi, J.; Liu, L.; Secret, E.; Chen, Y. Fabrication of polymer fiber scaffolds by centrifugal spinning for cell culture studies. *Microelectron. Eng.* **2011**, *88*, 1718–1721. [[CrossRef](#)]
142. Yanilmaz, M.; Lu, Y.; Zhu, J.; Zhang, X. Silica/polyacrylonitrile hybrid nanofiber membrane separators via sol-gel and electrospinning techniques for lithium-ion batteries. *J. Power Sources* **2016**, *313*, 205–212. [[CrossRef](#)]
143. Lu, Y.; Fu, K.; Zhu, J.; Chen, C.; Yanilmaz, M.; Dirican, M.; Ge, Y.; Jiang, H.; Zhang, X. Comparing the structures and sodium storage properties of centrifugally spun SnO₂ microfiber anodes with/without chemical vapor deposition. *J. Mater. Sci.* **2016**, *51*, 4549–4558. [[CrossRef](#)]
144. Taghavi, S.M.; Larson, R.G. Regularized thin-fiber model for nanofiber formation by centrifugal spinning. *Phys. Rev. E* **2014**, *89*, 023011. [[CrossRef](#)] [[PubMed](#)]
145. Padron, S.; Fuentes, A.; Caruntu, D.; Lozano, K. Experimental study of nanofiber production through forcespinning. *J. Appl. Phys.* **2013**, *113*, 024318. [[CrossRef](#)]
146. Loordhuswamy, A.M.; Krishnaswamy, V.R.; Korrapati, P.S.; Thinakaran, S.; Rengaswami, G.D.V. Fabrication of highly aligned fibrous scaffolds for tissue regeneration by centrifugal spinning technology. *Mater. Sci. Eng. C* **2014**, *42*, 799–807. [[CrossRef](#)]
147. Stojanovska, E.; Canbay, E.; Pampal, E.S.; Calisir, M.D.; Agma, O.; Polat, Y.; Simsek, R.; Gundogdu, N.A.S.; Akgul, Y.; Kilic, A. A review on non-electro nanofibre spinning techniques. *RSC Adv.* **2016**, *6*, 83783–83801. [[CrossRef](#)]
148. Fang, Y.; Dulaney, A.R.; Gadley, J.; Maia, J.; Ellison, C.J. A comparative parameter study: Controlling fiber diameter and diameter distribution in centrifugal spinning of photocurable monomers. *Polymer* **2016**, *88*, 102–111. [[CrossRef](#)]
149. Natarajan, T.S.; Bhargava, P. Influence of spinning parameters on synthesis of alumina fibres by centrifugal spinning. *Ceram. Int.* **2018**, *44*, 11644–11649. [[CrossRef](#)]
150. Stojanovska, E.; Kurtulus, M.; Abdelgawad, A.; Candan, Z.; Kilic, A. Developing lignin-based bio-nanofibers by centrifugal spinning technique. *Int. J. Biol. Macromol.* **2018**, *113*, 98–105. [[CrossRef](#)]
151. Zou, W.; Chen, R.Y.; Zhang, G.Z.; Zhang, H.C.; Qu, J.P. Recent advances in centrifugal spinning preparation of nanofibers. *Adv. Mater. Res.* **2014**, *1015*, 170–176. [[CrossRef](#)]
152. Szabó, P.; Sebe, I.; Stiedl, B.; Kállai-Szabó, B.; Zelkó, R. Tracking of crystalline-amorphous transition of carvedilol in rotary spun microfibers and their formulation to orodispersible tablets for in vitro dissolution enhancement. *J. Pharm. Biomed. Anal.* **2015**, *115*, 359–367. [[CrossRef](#)]
153. Marano, S.; Barker, S.A.; Raimi-Abraham, B.T.; Missaghi, S.; Rajabi-Siahboomi, A.; Craig, D.Q.M. Development of micro-fibrous solid dispersions of poorly water-soluble drugs in sucrose using temperature-controlled centrifugal spinning. *Eur. J. Pharm. Biopharm.* **2016**, *103*, 84–94. [[CrossRef](#)]
154. Yang, Y.; Zheng, N.; Zhou, Y.; Shan, W.; Shen, J. Mechanistic study on rapid fabrication of fibrous films via centrifugal melt spinning. *Int. J. Pharm.* **2019**, *560*, 155–165. [[CrossRef](#)]
155. Wang, L.; Chang, M.-W.; Ahmad, Z.; Zheng, H.; Li, J.-S. Mass and controlled fabrication of aligned PVP fibers for matrix type antibiotic drug delivery systems. *Chem. Eng. J.* **2017**, *307*, 661–669. [[CrossRef](#)]
156. Li, X.; Lu, Y.; Hou, T.; Zhou, J.; Yang, B. Centrifugally spun ultrafine starch/PEO fibres as release formulation for poorly water-soluble drugs. *Micro Nano Lett.* **2018**, *13*, 1688–1692. [[CrossRef](#)]
157. Cremer, L.; Gutierrez, J.; Martinez, J.; Materon, L.; Gilkerson, R.; Xu, F.; Lozano, K. Development of antimicrobial chitosan based nanofiber dressings for wound healing applications. *Nanomed. J.* **2018**, *5*, 6–14.
158. Xia, L.; Lu, L.; Liang, Y.; Cheng, B. Fabrication of centrifugally spun prepared poly(lactic acid)/gelatin/ciprofloxacin nanofibers for antimicrobial wound dressing. *RSC Adv.* **2019**, *9*, 35328–35335. [[CrossRef](#)]
159. Aydogdu, M.O.; Altun, E.; Ahmed, J.; Gunduz, O.; Edirisinghe, M. Fiber Forming Capability of Binary and Ternary Compositions in the Polymer System: Bacterial Cellulose–Polycaprolactone–Polylactic Acid. *Polymers* **2019**, *11*, 1148. [[CrossRef](#)]

160. Rampichová, M.; Buzgo, M.; Míčková, A.; Vocetková, K.; Sovková, V.; Lukášová, V.; Filová, E.; Rustichelli, F.; Amler, E. Platelet-functionalized three-dimensional poly- ϵ -caprolactone fibrous scaffold prepared using centrifugal spinning for delivery of growth factors. *Int. J. Nanomed.* **2017**, *12*, 347–361. [[CrossRef](#)]
161. Rampichová, M.; Lukášová, V.; Buzgo, M.; Vocetková, K.; Sovková, V.; Blahnová, V.; Amler, E.; Filová, E. Coaxial Nanofibrous Scaffold Prepared Using Centrifugal Spinning as a Drug Delivery System for Skeletal Tissue Engineering. *Key Eng. Mater.* **2020**, 162–168. [[CrossRef](#)]
162. Mamidi, N.; Zuníga, A.E.; Villela-Castrejón, J. Engineering and evaluation of forcespun functionalized carbon nano-onions reinforced poly (ϵ -caprolactone) composite nanofibers for pH-responsive drug release. *Mater. Sci. Eng. C* **2020**, *112*, 110928. [[CrossRef](#)]
163. da Silva Parize, D.D.; Foschini, M.M.; de Oliveira, J.E.; Klamczynski, A.P.; Glenn, G.M.; Marconcini, J.M.; Mattoso, L.H.C. Solution blow spinning: Parameters optimization and effects on the properties of nanofibers from poly (lactic acid)/dimethyl carbonate solutions. *J. Mater. Sci.* **2016**, *51*, 4627–4638. [[CrossRef](#)]
164. Behrens, A.M.; Casey, B.J.; Sikorski, M.J.; Wu, K.L.; Tutak, W.; Sandler, A.D.; Kofinas, P. In situ deposition of PLGA nanofibers via solution blow spinning. *ACS Macro Lett.* **2014**, *3*, 249–254. [[CrossRef](#)]
165. Dadol, G.C.; Kilic, A.; Tijing, L.D.; Lim, K.J.A.; Cabatingan, L.K.; Tan, N.P.B.; Stojanovska, E.; Polat, Y. Solution blow spinning (SBS) and SBS-spun nanofibers: Materials, methods, and applications. *Mater. Today Commun.* **2020**, *25*, 101656. [[CrossRef](#)]
166. Shi, S.; Zhuang, X.; Cheng, B.; Wang, X. Solution blowing of ZnO nanoflake-encapsulated carbon nanofibers as electrodes for supercapacitors. *J. Mater. Chem. A* **2013**, *1*, 13779–13788. [[CrossRef](#)]
167. dos Santos, D.M.; Correa, D.S.; Medeiros, E.S.; Oliveira, J.E.; Mattoso, L.H.C. Advances in Functional Polymer Nanofibers: From Spinning Fabrication Techniques to Recent Biomedical Applications. *ACS Appl. Mater. Interfaces* **2020**, *12*, 45673–45701. [[CrossRef](#)]
168. Medeiros, E.S.; Glenn, G.M.; Klamczynski, A.P.; Orts, W.J.; Mattoso, L.H. Solution blow spinning: A new method to produce micro-and nanofibers from polymer solutions. *J. Appl. Polym. Sci.* **2009**, *113*, 2322–2330. [[CrossRef](#)]
169. Oliveira, J.E.; Medeiros, E.S.; Cardozo, L.; Voll, F.; Madureira, E.H.; Mattoso, L.H.C.; Assis, O.B.G. Development of poly(lactic acid) nanostructured membranes for the controlled delivery of progesterone to livestock animals. *Mater. Sci. Eng. C* **2013**, *33*, 844–849. [[CrossRef](#)]
170. Souza, M.A.; Sakamoto, K.Y.; Mattoso, L.H.C. Release of the Diclofenac Sodium by Nanofibers of Poly(3-hydroxybutyrate-co-3-hydroxyvalerate) Obtained from Electrospinning and Solution Blow Spinning. *J. Nanomater.* **2014**, *2014*, 129035. [[CrossRef](#)]
171. Bonan, R.F.; Bonan, P.R.F.; Batista, A.U.D.; Sampaio, F.C.; Albuquerque, A.J.R.; Moraes, M.C.B.; Mattoso, L.H.C.; Glenn, G.M.; Medeiros, E.S.; Oliveira, J.E. In vitro antimicrobial activity of solution blow spun poly(lactic acid)/polyvinylpyrrolidone nanofibers loaded with Copaiba (*Copaifera* sp.) oil. *Mater. Sci. Eng. C* **2015**, *48*, 372–377. [[CrossRef](#)]
172. Balogh, A.; Farkas, B.; Faragó, K.; Farkas, A.; Wagner, I.; Verreck, G.; Nagy, Z.K.; Marosi, G. Melt-blown and electrospun drug-loaded polymer fiber mats for dissolution enhancement: A comparative study. *J. Pharm. Sci.* **2015**, *104*, 1767–1776. [[CrossRef](#)] [[PubMed](#)]
173. Heseltine, P.L.; Ahmed, J.; Edirisinghe, M. Developments in pressurized gyration for the mass production of polymeric fibers. *Macromol. Mater. Eng.* **2018**, *303*, 1800218.
174. Raimi-Abraham, B.T.; Mahalingam, S.; Davies, P.J.; Edirisinghe, M.; Craig, D.Q. Development and characterization of amorphous nanofiber drug dispersions prepared using pressurized gyration. *Mol. Pharm.* **2015**, *12*, 3851–3861. [[CrossRef](#)] [[PubMed](#)]
175. Brako, F.; Raimi-Abraham, B.T.; Mahalingam, S.; Craig, D.Q.M.; Edirisinghe, M. The development of progesterone-loaded nanofibers using pressurized gyration: A novel approach to vaginal delivery for the prevention of pre-term birth. *Int. J. Pharm.* **2018**, *540*, 31–39. [[CrossRef](#)]
176. Cam, M.E.; Hazar-Yavuz, A.N.; Cesur, S.; Ozkan, O.; Alenezi, H.; Turkoglu Sasmazel, H.; Sayip Eroglu, M.; Brako, F.; Ahmed, J.; Kabasakal, L.; et al. A novel treatment strategy for preterm birth: Intra-vaginal progesterone-loaded fibrous patches. *Int. J. Pharm.* **2020**, *588*, 119782. [[CrossRef](#)]
177. Ahmed, J.; Matharu, R.K.; Shams, T.; Illangakoon, U.E.; Edirisinghe, M. A Comparison of Electric-Field-Driven and Pressure-Driven Fiber Generation Methods for Drug Delivery. *Macromol. Mater. Eng.* **2018**, *303*, 1700577. [[CrossRef](#)]
178. Ahmed, J.; Altun, E.; Aydogdu, M.O.; Gunduz, O.; Kerai, L.; Ren, G.; Edirisinghe, M. Anti-fungal bandages containing cinnamon extract. *Int. Wound J.* **2019**, *16*, 730–736. [[CrossRef](#)]
179. Cam, M.E.; Yildiz, S.; Alenezi, H.; Cesur, S.; Ozcan, G.S.; Erdemir, G.; Edirisinghe, U.; Akakin, D.; Kuruca, D.S.; Kabasakal, L.; et al. Evaluation of burst release and sustained release of pioglitazone-loaded fibrous mats on diabetic wound healing: An in vitro and in vivo comparison study. *J. R. Soc. Interface* **2020**, *17*, 20190712. [[CrossRef](#)]
180. Cam, M.E.; Ertas, B.; Alenezi, H.; Hazar-Yavuz, A.N.; Cesur, S.; Ozcan, G.S.; Ekentok, C.; Guler, E.; Katsakouli, C.; Demirbas, Z.; et al. Accelerated diabetic wound healing by topical application of combination oral antidiabetic agents-loaded nanofibrous scaffolds: An in vitro and in vivo evaluation study. *Mater. Sci. Eng. C* **2021**, *119*, 111586. [[CrossRef](#)]
181. Altun, E.; Aydogdu, M.O.; Koc, F.; Crabbe-Mann, M.; Brako, F.; Kaur-Matharu, R.; Ozen, G.; Kuruca, S.E.; Edirisinghe, U.; Gunduz, O.; et al. Novel Making of Bacterial Cellulose Blended Polymeric Fiber Bandages. *Macromol. Mater. Eng.* **2018**, *303*, 1700607. [[CrossRef](#)]
182. Qi, S.; Craig, D. Recent developments in micro-and nanofabrication techniques for the preparation of amorphous pharmaceutical dosage forms. *Adv. Drug Deliv. Rev.* **2016**, *100*, 67–84. [[CrossRef](#)] [[PubMed](#)]

183. Luo, C.; Stoyanov, S.D.; Stride, E.; Pelan, E.; Edirisinghe, M. Electrospinning versus fibre production methods: From specifics to technological convergence. *Chem. Soc. Rev.* **2012**, *41*, 4708–4735. [[CrossRef](#)]
184. Brown, T.D.; Dalton, P.D.; Hutmacher, D.W. Melt electrospinning today: An opportune time for an emerging polymer process. *Prog. Polym. Sci.* **2016**, *56*, 116–166. [[CrossRef](#)]
185. Cheng, J.; Jun, Y.; Qin, J.; Lee, S.-H. Electrospinning versus microfluidic spinning of functional fibers for biomedical applications. *Biomaterials* **2017**, *114*, 121–143. [[CrossRef](#)] [[PubMed](#)]
186. Wang, F.; Li, Z.; Tamama, K.; Sen, C.K.; Guan, J. Fabrication and characterization of pro-survival growth factor releasing, anisotropic scaffolds for enhanced mesenchymal stem cell survival/growth and orientation. *Biomacromolecules* **2009**, *10*, 2609–2618. [[CrossRef](#)]
187. Zhu, W.; Masood, F.; O'Brien, J.; Zhang, L.G. Highly aligned nanocomposite scaffolds by electrospinning and electrospaying for neural tissue regeneration. *Nanomed. Nanotechnol. Biol. Med.* **2015**, *11*, 693–704. [[CrossRef](#)]
188. Birajdar, M.S.; Lee, J. Sonication-triggered zero-order release by uncorking core-shell nanofibers. *Chem. Eng. J.* **2016**, *288*, 1–8. [[CrossRef](#)]
189. Nagy, Z.K.; Balogh, A.; Drávavölgyi, G.; Ferguson, J.; Pataki, H.; Vajna, B.; Marosi, G. Solvent-Free Melt Electrospinning for Preparation of Fast Dissolving Drug Delivery System and Comparison with Solvent-Based Electrospun and Melt Extruded Systems. *J. Pharm. Sci.* **2013**, *102*, 508–517. [[CrossRef](#)]
190. Balogh, A.; Drávavölgyi, G.; Faragó, K.; Farkas, A.; Vigh, T.; Sóti, P.L.; Wagner, I.; Madarász, J.; Pataki, H.; Marosi, G.; et al. Plasticized Drug-Loaded Melt Electrospun Polymer Mats: Characterization, Thermal Degradation, and Release Kinetics. *J. Pharm. Sci.* **2014**, *103*, 1278–1287. [[CrossRef](#)]
191. Lian, H.; Meng, Z. Melt electrospinning vs. solution electrospinning: A comparative study of drug-loaded poly (ϵ -caprolactone) fibres. *Mater. Sci. Eng. C* **2017**, *74*, 117–123. [[CrossRef](#)]
192. Balogh, A.; Horváthová, T.; Fülöp, Z.; Loftsson, T.; Harasztos, A.H.; Marosi, G.; Nagy, Z.K. Electroblowing and electrospinning of fibrous diclofenac sodium-cyclodextrin complex-based reconstitution injection. *J. Drug Deliv. Sci. Technol.* **2015**, *26*, 28–34. [[CrossRef](#)]
193. Sóti, P.L.; Bocz, K.; Pataki, H.; Eke, Z.; Farkas, A.; Verreck, G.; Kiss, É.; Fekete, P.; Vigh, T.; Wagner, I.; et al. Comparison of spray drying, electroblowing and electrospinning for preparation of Eudragit E and itraconazole solid dispersions. *Int. J. Pharm.* **2015**, *494*, 23–30. [[CrossRef](#)]
194. Ahn, S.; Mun, C.; Lee, S.H. Microfluidic spinning of fibrous alginate carrier having highly enhanced drug loading capability and delayed release profile. *RSC Adv.* **2015**, *5*, 15172–15181. [[CrossRef](#)]

Disclaimer/Publisher's Note: The statements, opinions and data contained in all publications are solely those of the individual author(s) and contributor(s) and not of MDPI and/or the editor(s). MDPI and/or the editor(s) disclaim responsibility for any injury to people or property resulting from any ideas, methods, instructions or products referred to in the content.